Archives of Current Research International

9(2): 1-35, 2017; Article no.ACRI.35252
ISSN: 2454-7077

Mechanical and Acoustic Emission Behavior of Mg-Li Based Alloys Compressed Before and After Pre-Deformation by Intensive Strain Methods

Andrzej Pawełek[1*]

[1]Polish Academy of Sciences, Aleksander Krupkowski Institute of Metallurgy and Materials Science, 30-059 Cracow, Reymonta St. 25, Poland.

Author's contribution

The sole author designed, analyzed and interpreted and prepared the manuscript.

Article Information

DOI: 10.9734/ACRI/2017/35252
Editor(s):
(1) Wang Mingyu, School of Metallurgy and Environment, Central South University, China.
Reviewers:
(1) Emilio Jiménez, University of La Rioja, Spain.
(2) Hua Zhang, Taiyuan University of Technology, China.
(3) Qiang Li, Shenyang University of Technology, China.
Complete Peer review History: http://www.sciencedomain.org/review-history/20826

Review Article

Received 3rd July 2017
Accepted 15th August 2017
Published 5th September 2017

ABSTRACT

The behavior of acoustic emission (AE) and its relationships with mechanisms of compression deformations of Mg-Li and Mg-Li-Al based alloys before and after the processing by intensive strain methods such as the ECAP (Equal Channel Angular Pressing) and the HPT (High Pressure Torsion) was examined. It was shown that the AE behaviour may be explained in terms of the collective, highly synchronized movements of the groups of many dislocations related to their acceleration as well as internal and surface annihilation.
The intensity of AE in α single-phase of Mg-4Li based alloys is almost two orders of magnitude higher than that in pure Mg, and AE event rate reaches the maximum for Mg4Li alloy, what is imposed by the effect of Li addition, in leading to favoring of additional slip systems in prismatic and pyramidal planes. On the other hand the AE intensity in α+β two-phase of Mg-8Li based alloys rapidly decrease in comparison to that of single α phase. This is caused by very high diffusivity of lithium, which in consequence leading limitation the ability of dislocations to collective behavior. However, the AE intensity and activity in β single-phase of Mg-12Li based alloys is drastically low in comparison to α and α+β alloys. Two ranges of AE activity, observed in Mg12Li, is caused by high diffusivity of Li, which facilitating the processes of internal stress relaxation ensures generally

**Corresponding author: Email: a.pawelek@imim.pl;*

high plasticity of β single-phase alloys. Moreover, the investigations of Mg9Li-Al based alloys have showed, that the AE increases together with the increase of Al concentration is the result of growing volume contribution of very efficient acoustically hexagonal α phase.
The visible decrease of AE intensity and activity as well as increase in strength of alloys subjected to HPT and ECAP processing has been observed. Simultaneously the microstructure refinement of alloys after intensive strain processing was confirmed by electron (TEM) and optical microscopy technique. The possible explanation is discussed in terms of high increase of the density of immobile dislocations which strongly restrict ability to collective movement of source generate new dislocations. Also the hypothesis of possible contribution of slip along grain boundaries is discussed.

Keywords: Mg–Li alloys; acoustic emission; compression test; ultra fine grained (UFG) structures; dislocations.

1. INTRODUCTION

In the last decade a considerable attention has been given to obtaining nanocrystalline materials on account of their excellent mechanical properties, such as great strength and plasticity or even superplasticity occurring in condition of relatively not high temperatures [1]. The methods of intensive deformation have become more and more widely used to obtain microstructure refinement as they allow to obtain massive samples of metals ready for further treatment. This refers to packed rolling with bonding, the so called ARB (Accumulative Roll Bonding) method [2]. There is also known the ECAP (Equal Channel Angular Pressing) method of compression in angular channel [3-5]. Next the HPT (High Pressure Torsion) method of torsion under high pressure [1,5-7] is the least known since obtaining the high pressure alone is a difficult problem technically. The methods mentioned above are used for the refinement of the microstructure to obtain ultrafine or nanocrystalline grain size leading to the increase of strength and ductility of the material.

Alloys based on magnesium with lithium, as the lightest from among the known metallic construction materials, are very attractive materials from the point of view of their application as the materials for light, yet durable constructions for example in the automotive industry (e.g. car engine housings) or aerospace (e.g. light housings of computers). The basic Mg-Li alloys exist in three phase areas (Fig. 1.1). The hexagonal α phase appears in the concentration range of Li up to 4 wt.%. If the content of Li is more than 12 wt.% - the β phase of cubic lattice exists. The alloys of Li content from 4% up to 12 wt.% form α+β two-phase mixture.

Mechanical properties of α phase become worse than β phase which is more plastic and thus is characterized by good machinability and weldability. Alloying additions e.g. Al (or Cd, Zn or Si) from 3% to 5%, slightly increase the density of the alloy, but lead to the precipitation of coherent particles of transition phase, θ-$MgLi_2Al$, which additionally strengthens the matrix and leads to the improvement of mechanical properties [8].

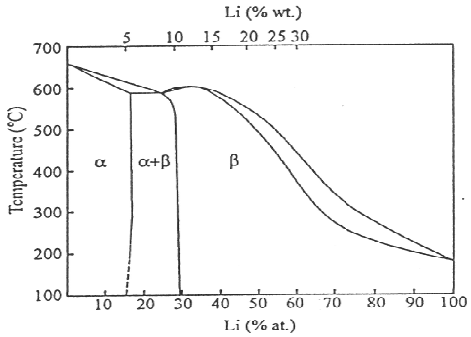

Fig. 1.1. A scheme of phase-diagram of magnesium-lithium system.

On the other hand the phenomenon of acoustic emission (AE) has long been known as the audible to the human ear sounds accompanying cracking of materials (e.g. Tin) or shifts of a medium. The first application of the AE method was monitoring the movements of the ground. However, it was discovered in the fiftieth years of XX century [9,10] that AE signals are generated also in metals under the action of mechanical load. This fact has opened, in the next few decades, a wide field for the research of practical application of the AE methods to monitoring the formation and development of structure cracking in metallic materials under the influence of growing external loads. This topic was widely

discussed in work [10]. It appeared that the mechanism of AE signal generation is very complex. It requires comprehensive research, but gives an unique resource of information on micro- and macroprocesses occurring in materials. Therefore it has become necessary to support the experimental studies and technical solutions with the fundamentals of the effect.

According to our knowledge there are no reports on the application of AE method to investigate the mechanical properties of Mg-Li alloys by using the channel-die test. The aim of the research has been the documentation and interpretation of correlation of the AE descriptors during compression tests of Al alloys before and after pre-deformation by intensive strain methods. The evolution of micro- and/or nanostructure in dependence on dislocation mechanisms of deformation as well as slip processes occurring along grain boundaries, responsible for possible superplastic flow, is also considered. However, at initial stage of investigations the discussion of the possible relations between AE and superplasticity has a preliminary character and it has been here carried out first on the basis of the measurement results of the most often used parameters of AE signals: i.e. RMS (Root Mean Square) and both the count number and energy of AE events.

The purpose of this work is also an attempt to show that the AE effects observed in channel-die compressed Mg-Li based alloys can be quite satisfactorily explained in terms of the collective and synchronized behavior of many groups of dislocations generally associated with the acceleration and both internal as well as surface annihilation of many dislocations.

2. EXPERIMENTAL PROCEDURES

The Mg-Li and Mg-Li-Al alloys were prepared in cooperation with the Institute of Materials and Machine Mechanics of the Slovak Academy of Sciences in Bratislava. The basic Mg-Li alloys were obtained by the method of induction melting of magnesium of 99.99% purity and lithium of 99.5% purity. Series of Mg-Li and Mg-Li-Al alloys used in this study were prepared by casting of raw materials in a steel crucible at 800°C with subsequent pouring into a cooled steel mould in a chamber of vacuum induction furnace (Balzers) under low argon pressure (1000Pa, of 99.999% purity) after previous evacuation (10^{-2}Pa). The applied preparation procedure was similar to that reported in [11] and used also in our previous works [12-14].

Samples of alloys before and after ECAP and HPT operations were subjected to compression tests in a testing machine of INSTRON type. The traverse speed of the testing machine was mostly equal to 0.05mm/min. Simultaneously with the registration of the external force and the sample elongation, the basic AE parameters in the form of AE event rate (count number), amplitude, duration and energy of single AE events as well as (more rarely) RMS value (effective voltage of AE signal) – could be potentially measured. A broad-band piezoelectric sensor (standard WD type, certified by Physical Acoustics Corporation) enabled to record the acoustic pulses in the frequency range from 100 kHz to 1MHz. The contact between the detector and the sample was maintained by means of a steel rail in a channel-die which formed a natural wave-guide. The amplification of the AE analyzer was 86dB and the threshold voltage of the discriminator was 1.17-1.20 V. In order to minimize the undesired effect of friction against the channel walls, each sample was covered with a Teflon foil. Moreover, before and after compression test, there have been carried out microstructure observations using the standard technique of optical, scanning (SEM) and/or electron (TEM) microscopy.

2.1 Chanel-die Compression Tests

The initial samples before HPT and ECAP treatment of Mg-Li and Mg-Li-Al of dimensions 10x10x10mm were cut out and subjected to tests of channel-die compression at room temperature using the new INSTRON-3082 testing machine equipped additionally with channel-die (Fig. 2.1), which ensured plastic flow merely in the normal direction ND (KN) and in the elongation direction ED (KW), parallel to the channel axis, since the deformation in the transverse direction TD (KP) was held back by the channel walls.

The channel-die compression test ensures the realization of planar state of deformation because the strain in the direction perpendicular to the channel walls do not exist. Therefore this test is better than the usual compression test or a rolling test, in which a more complex, three dimensional deformation occurs. Moreover, a higher deformation degree than in the traditional tensile test is achieved in the compression tests, which creates possibilities for better recognizing the mechanisms of deformation.

2.2 Methods of Intensive Deformation

Fig. 2.2a shows the scheme of the ECAP method. The parameters of the installation have the following values: *b*=10 mm, *a*=30 mm, angle α=31.3° or α=0° (for α=90° the sample is extruded out directly). Equivalent strain (for square cross-section) is equal to ε_n=0.5922*n*, where *n* – number of passes. For angle Φ= 90° and α=0° it amounts to ε_n=0.9069*n*. Fig. 2.2b shows the scheme of the HPT method of torsion under high pressure. The sample is in the form of a roll with *R* radius and the height *l*. Dilatation strain *γ* after *N* rotations is equal to $\gamma=(2\pi RN)/l$, and the equivalent strain $\varepsilon_N=\gamma/1.73$.

The program of angle channel extrusion referred mainly to the Mg8Li alloy. The process of extrusion with the use of equal channel angular pressing ECAP was carried out for the samples of circular cross sections. The samples of 13 mm radius and 60 mm length were machined in Institute of Materials and Machine Mechanics of Slovak Academy of Sciences. The samples were processed in Accredited Laboratory of Strength of Materials at the Institute of Metallurgy and Materials Science of Polish Academy of Sciences. An INSTRON-3382 testing machine of maximal load 100kN and an angular channel of 13 mm radius and 90° bend angle was used for the extrusion of samples. The samples were

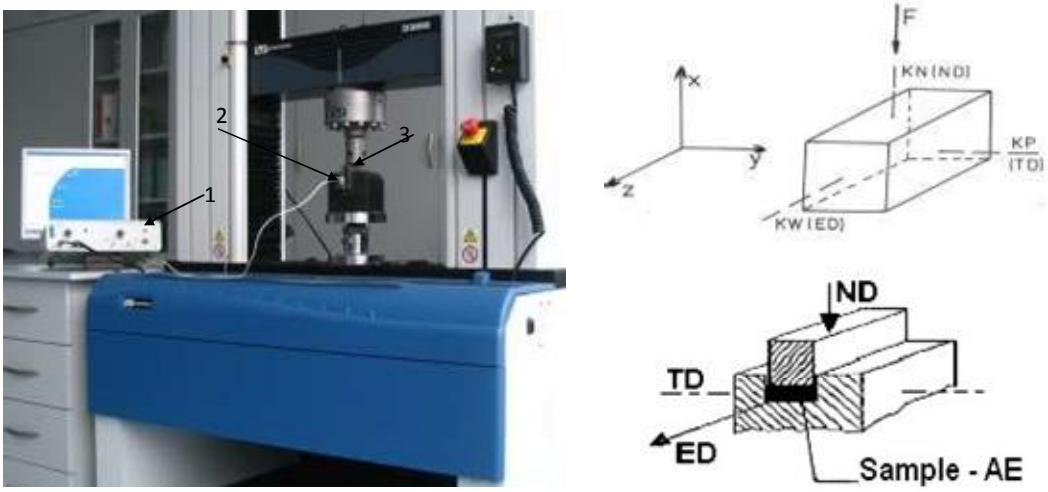

Fig. 2.1. The experimental set-up used to record the AE signals generated in compressed samples: 1 – AE analyzer, 2 - AE sensor, 3 – Channel-die used as a sample holder.

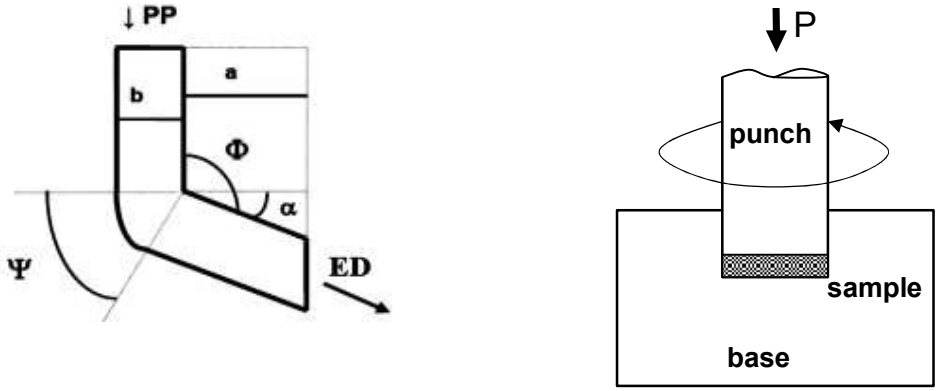

(a) **(b)**

Fig. 2.2. (a) – scheme of ECAP angular extrusion: ED – direction of outflow, PP – direction of the punch pressure, and (b) – the scheme of the HPT process.

deformed at constant rate of traverse v=0.8 mm/min at 100°C along route B, i.e. after each pass, the samples were rotated by 90° around the extrusion direction and processed again. The Mg8Li samples were passed 2, 3 and 4 times.

On the other hand the samples to be used for the ECAP processing in the channel of square cross section was in the shape of rectangular prisms of dimensions 10x10x40 mm. The samples to be used in HPT tests had the shape of disks of the diameter 13 mm and the thickness of the order of 2-3 mm. Samples intended for compression had the shape of cubes with the edge not greater than 10 mm in case of ECAP or the shape of square plates with the side 10 mm and the thickness of the order of 1-2 mm in the case of HPT. The channel-die compression tests were realized using the same INSTRON-3382 machine as for ECAP operations. The traverse rate of the machine in the compression tests was 0.05 mm/min, and in the ECAP tests it was 0.8 mm/min.

Samples intended for compression test before HPT operations, besides of cubic shape of 10 mm side, had also the shape of square plates of the side of 10 mm and also the thickness of the order of 2-3 mm. After large plastic deformation, intended for further compression tests, thickness was similarly in the range 1-2 mm. Samples for mechanical-acoustic testing had small dimensions – smaller than diameter of AE transducer. Additionally, AE signals emitted during compression were characterized by low energy, only a little higher than background noise. It was important to solve problem of registering acoustic emission activity of the samples during compressive force increase.

2.3 Acoustic Emission Technique

AE takes place during rapid release of elastic energy accumulated in the material as a result of acting external incentives or internal conversions. External mechanical, thermal, chemical or radiation interactions can cause deformational processes during which part of accumulated energy can be emitted in form of elastic waves. Areas of the material, where deformation processes take place, become the source of AE effects. The frequency of acoustic waves is in range between several kilohertz and a few megahertz. They are generated as the effect of initiation and growth of microcracks, local dislocations movement, internal friction, chemical reactions, phase transitions and internal electric discharges in pores or discontinuities. AE method enables sensitive monitoring effects in real time, even in considerable volume of investigated elements. It is possible to detect crack effects under minor stress condition, which can be hardly monitored using other methods. The varying intensity of AE signals enables studying the behavior of investigated metal alloys under mechanical load. Important fact is that evolution of the material microstructure due to external stresses which lead to the changes of the emitted AE signals.

The analytical description of propagation of AE signal in real object is very complex. The phenomena causing the modification of propagating wave modes are reflections and transformations at the borders of the regions characterized by different acoustic impedance.

However, the AE wave propagation for the region situated far from the source in homogenous medium can be described using the Green function. Basing on the simplified assumptions, that the function of strain field amplitude has a form of a unique jump, the observation point is in a far away area, while the elastic wave propagates in homogeneous medium, the elementary equation of signal propagation way can be described with the following relation [15]:

$$G(x,t'-t;x)=\frac{1}{4\pi\rho v_p^2}\gamma_i\gamma_j\frac{1}{r}\delta(t'-t-r'/v_p)-\frac{1}{4\pi\rho v_s^2}(\gamma_i\gamma_j-\delta_{ij})\frac{1}{r}\delta(t'-t-r'/v_s)$$

where: $G_{ij}(\boldsymbol{r}',t'-t;\boldsymbol{r})$ is Green function for the displacement in directions $\mathbf{x}'_i$, $\mathbf{y}'_i$, $\mathbf{z}'_i$ in time t', for the case when a local distortion of strain field in point $\boldsymbol{r}$ in time t is the source of these displacements, ρ - medium density [kg/m^3], v_p – rate of dilatational wave, v_s – velocity of shear wave, γ_i, γ_j - for i = 1, 2, 3, j = 1, 2, 3 are directional cosines source-receiver and receiver-source, r – distance between AE source and sensor, δ_{ij} – Kronecker's delta, $\delta(x)$ –delta function, equal $+\infty$ for x=0 and equal 0 for other values x.

The output signal is converted into voltage and amplified with a low-noise charge sensitive preamplifier. A full-wave rectifier drives the integrator at the output of which an envelope of a single AE pulse is obtained. The signals from the mean-value detector are transmitted directly to the voltage discriminator, each of them which exceeds the threshold level being counted only once, which corresponds to a single recorded AE event.

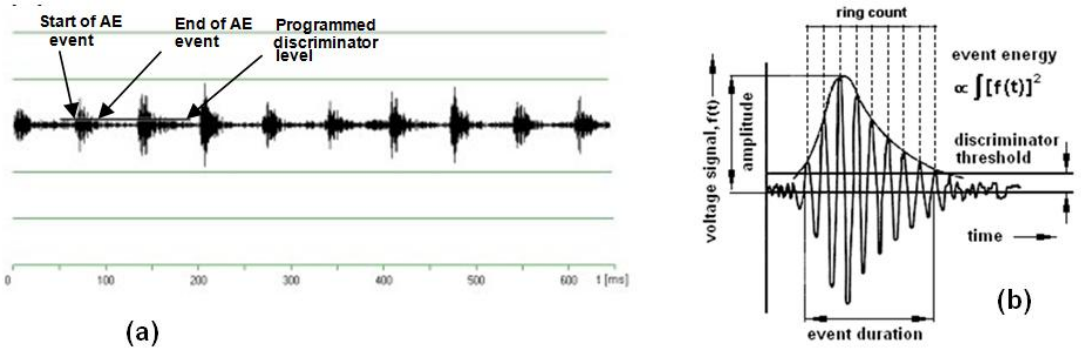

Fig. 2.3. Principle of detection of AE events (a), and basic parameters of a single event (b).

AE analyzer enables a simultaneous registration of external compression force as well as recording of AE parameters in the form of course of events, their amount and energy and also the energy of an individual AE events, their amplitude and duration resulting in establishing the AE energetic spectrum, acoustic maps (spectrograms or acoustograms) and spectral dependences of number of events on energy of recorded AE events. Multi-parameter spectral analysis of AE signals is necessary for the identification of individual mechanisms of plastic deformations.

Apart from the AE signal, the apparatus registers also noise of the acoustic background and the noise generated in the course of processing of the registered signal.

A line determining the maximal level of noise voltage of environment background is shown in Fig. 2.3. The level is named “discrimination voltage”. The occurrence of AE event is defined as a moment of an instantaneous increase of signal value above the discrimination voltage and the duration time of AE event is determined to the moment of the decrease of instantaneous signal value below the discrimination voltage.

The *sampling period of the analogue-numerical converter* is the significant factor affecting the level of the instrument sensitivity with regards to the AE signal analysis. This is why, a fast card of the analogue-numerical converter of 9812 ADLINK was used when completing the AE signal analysis system. The device has possibility to change sampling frequency in the range 0.001-20 Msamples/s, 12-bits resolution and a library of maintenance procedures convenient for implementation at designing the software for measurement procedures. The application of the analogue-numerical converter card together with modern software enabled the increase of sensitivity of device detecting the AE events by an order of magnitude. The start and end indexes recorded in the program table of AE events can serve for the determination of duration time of AE event. Its *E* energy can be obtained from an approximate formula:

$$E = 0.5\, v^2_{max} \bullet \Delta t,$$

where v_{max} denotes maximal value of AE signal during the event, and Δt – its duration time.

In order to characterize a material subjected to the examinations with the AE technique, the values of arithmetic means of all measured quantities *E,* v_{max} and Δt should be given. The AE device is also equipped with an analogue system determining the effective value of the AE signal. The transformation of the set of instantaneous values of measured signal *v(t)* into effective value V_{RMS} for time T is realized according to formula:

$$V_{RMS} = \sqrt{\frac{1}{T}\int_0^T v^2(t)dt}$$

The differences of the AE signal generated by various sources in an object can be analyzed examining changes of its *spectrum characteristics*. Continuous AE signal *v*(*t*) in a selected finished range of time can be presented as a function of its spectral characteristic $A(\omega)$, where ω is frequency pulsation *f,* described as $\omega=2\pi f$. Assuming absolute integrability, function *v*(*t*), is linearly transformed into spectral density $A(\omega)$ according to the formula below (Fourier transformation):

$$v(t) = \frac{1}{\pi}\int_0^{\infty} A(\omega)\exp(\ j\omega\ )\,d\omega\ .$$

The new procedure of determination of spectral density function $A(\omega)$ for subsequent segments

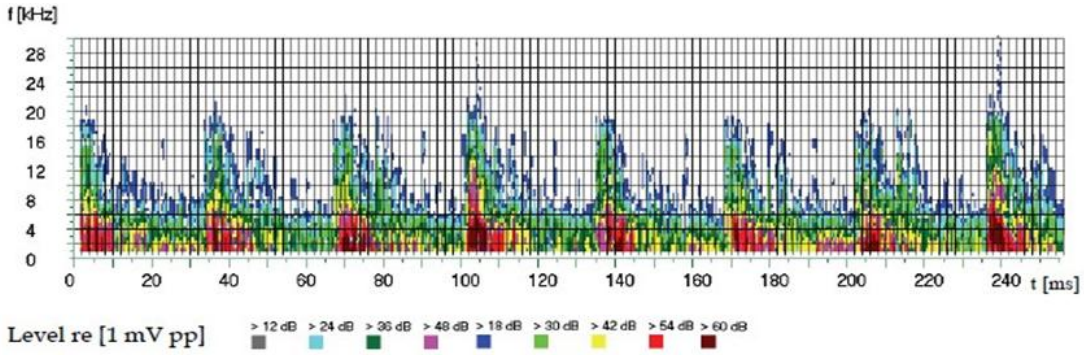

Fig. 2.4. Acoustogram of AE event set as a function of frequency on time.

of discrete set of AE signal samples together with a corresponding graphic presentation of results is introduced in this work. A method of window digital Fourier transformation (STFT) will be applied here. Next a discrete form of spectral density function is determined. The formula to transform the set of signal samples into a set of spectral density factors $c_n : v(m) \Rightarrow c_n(\omega)$ has an approximate form [9]:

$$c_n \approx \frac{1}{N} \sum_{m=0}^{N-1} v(m) \cdot \mathrm{mod}(e^{jn2\pi m/N}),$$

where j denotes imaginary unit, and a mod – module of complex expression.

The spectrogram (acoustogram) of AE event set, which was earlier shown as a signal characteristic is shown in Fig. 2.4 every 0.5msec. The discrete equivalent of spectral density function $A(\omega)$ is illustrated in the form of color code.

The software, partially improved by the authors, enabled first attempts to identify the AE sources based on distributions of AE event quantity as a function of discrimination level [16]. The broad-band piezoelectric sensor allowed recording the acoustic impulses in frequency range from 100kH to 1MHz. The contact of sensor and sample was maintained with the use of a steel rail as a washer in the channel die, which served as an acoustic wave-guide. It was an innovating solution of problem of AE sensor and compressed sample contact. Moreover, in order to eliminate undesirable effects of friction against the channel walls, each sample was covered with Teflon foil. The traverse rate of testing machine during the channel-die compression was almost always the same (0.05mm/min) for the metal and alloys examined.

The results of measurements were obtained using the new Acoustic Emission analyzer, which allowed to plot of both the spectrograms and the spectral characteristics produced with the application of Windowed Fourier Transform method for analysis of large experimental data sets. The results are compared with those obtained for similar materials but not subjected to intensive strain processing and the AE behavior is discussed in the dislocation aspects of both the theoretical concepts of Acoustic Emission sources and the plastic strain mechanisms (including possible superplastic flow) in ultra-fine grained or nanocrystalline materials.

3. RESULTS AND DISCUSSION

3.1 AE in Single α-phase Alloys Based on *hcp* Matrix

3.1.1 Polycrystalline Mg and Mg4Li based alloys

The starting point for the discussion of the AE and deformation mechanisms in Mg-Li alloys is their recognition in mono- and polycrystalline Mg. It is well known that the predominant deformation mechanisms in Mg single crystals are related to the operation of three slip systems: the basal {1000}<11 $\bar{2}$0>, the prismatic {10 $\bar{1}$ 0}<11 $\bar{2}$0> and the pyramidal one {10 $\bar{1}$ 1}<11 $\bar{2}$0>. These systems are also dominating in the polycrystalline Mg. The behavior of AE in polycrystalline Mg, as it was observed in our earlier paper [13], is typical as it is in other metals [10,15,17,18] and in the most cases it is characterized by large maximum of AE intensity within the range of yield point (including the microplasticity) and the successive decrease with the progress of the work hardening process. Generally, the opinion prevails that the AE

maximum in pure metals is related with the operation of the dislocation sources in the favored oriented slip systems, though the various forms of dislocation movements are especially considered as the dominating AE sources. Particularly, our earlier investigations [17,19-24] strongly suggest that the more essential contribution to the detected AE signals originates from the acceleration of the collective movement of the dislocation groups as well as from the annihilation processes of many coplanar dislocations which occur inside and at the free surface of the deformed sample. These are mostly groups of many simultaneously acting slip systems, which form, as result, slip lines, slip bands or finally shear bands. The role of the sample surface in AE phenomenon is strongly suggested also by other researches (e.g. Vinogradov [25]). In the case of Mg the AE activity is determined by the dominating generation of dislocations in the basal slip systems and the observed maximum of the rate of AE events attains the values of the order of $3x10^4/3s \cong 10^4/s$, as it show on Fig. 3.1a (see also in [13]).

Fig. 3.1 shows the AE and external compression force behavior in pure polycrystalline magnesium (99.99%) before (Fig. 3.1a) and after ECAP processing (Fig. 3.1b), since they contribute to its basic mechanical and acoustic description, to which the further results for alloys based on Mg-Li matrix will be referred to.

A drastically different level of AE activity is observed in single-phase α-Mg4Li alloy of *hcp* structure (Fig. 3.2a). It is very high and attains the value $5x10^6/4s \cong 1.3x10^6/s$, i.e. over two orders of magnitude higher than in Mg (Fig. 3.1a). It is due to the influence of lithium which considerably reduces the ratio **c/a** of the lattice parameters which favors the possibility of the activation of new slip systems in which both prismatic and pyramidal planes are additionally active. The variety of slips is illustrated with the image of microstructure of the deformed alloy (Fig. 3.2b). Moreover, one can see that the addition of Al (Fig. 3.3) leads to the distinct increase of the strengthening and to the decrease of AE by nearly three times in comparison with Mg4Li.

The level of AE activity in Mg4Li3Al and Mg4Li5Al alloys (Fig. 3.3a,b respectively) though considerably smaller than in Mg4Li alloy (Fig. 3.2a), is still very high, of the order of $1.5x10^6/4s \approx 4x10^5/s$ in comparison with that in pure Mg (Fig. 3.1). The expected increase of strengthening with increasing Al content in theses alloys is confirmed by the increasing values of the maximal external forces. It seems that the Al addition results in the decrease of AE level nearly by one order of the magnitude in comparison with pure Mg4Li alloy.

It is also characteristic observation that the AE level of intensity increases a little but visibly with the rise of Al alloying addition concentration. The influence of Al content on AE will be precisely examined in the next part 3.2 on diphase Mg8Li and Mg9Li alloys, in which its interpretation and explanation will be proposed.

The three-component Mg-Li-Al alloys can be hardened by ageing in the result of the formation of stable LiAl particles, which is preceded with the appearance of metastable, coherent $MgLi_2Al$ precipitates of θ metastable phase (of Guinier-Preston type). These are the most probable reasons for the increase of strength of single-phase Mg4Li5Al alloys and, which follows, the drop of AE event rate level due to the constraint of collective action of dislocation groups in the solid solution compared to pure Mg4Li alloy, in which dislocation processes are prevailing part of physical reasons for the AE occurrence.

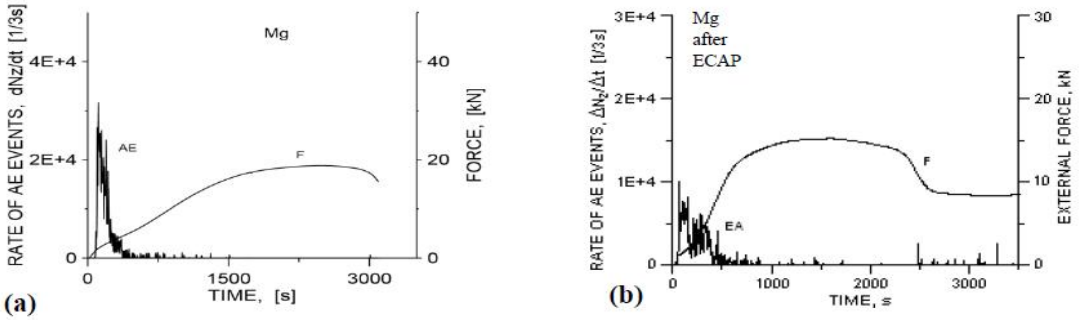

Fig. 3.1. AE in channel-die compressed pure (99.99%) polycrystalline magnesium: (a) – before and (b) – after 1x-ECAP operation.

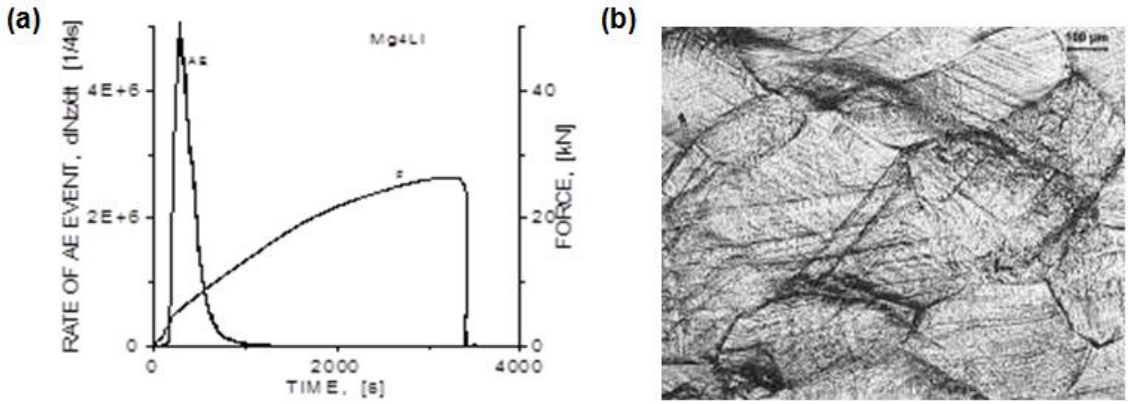

Fig. 3.2. EA in single phase α-Mg4Li alloy (a) and the corresponding microstructure (b) after deformation.

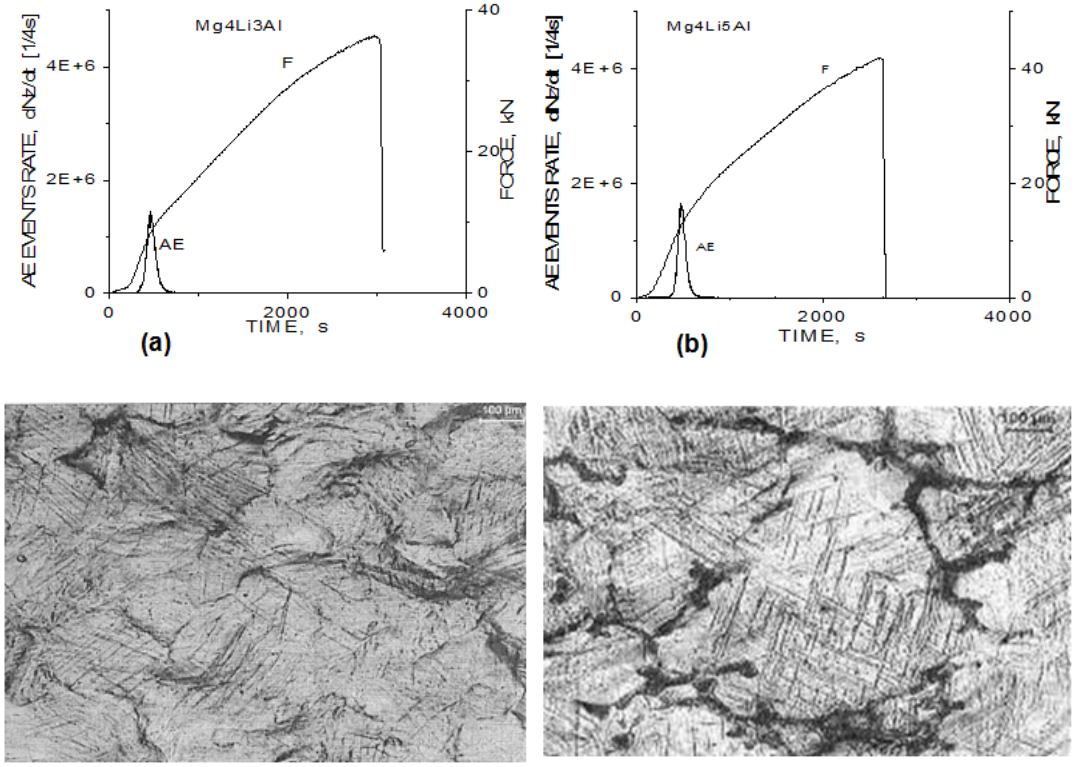

Fig. 3.3. AE in Mg4Li3Al (a) and Mg4Li5Al (b) alloys together with relevant, typical optical microstructures after deformation (below).

3.2 AE in (α+β) Diphase Alloys Based on Mixed *hcp* and *cubic* Matrix

3.2.1 Mg8Li, Mg8Li3Al and Mg8Li5Al alloys

A quite different AE behavior is observed in diphase (α+β)-Mg8Li alloy (Fig. 3.4a). The level of the AE activity (~$8x10^4$/4s≡$2x10^4$/s) is intermediate between that in Mg and Mg4Li alloy. Such AE behavior can be attributed to the influence of β phase which is responsible for the improvement of the plasticity of Mg8Li alloys (the sample did not fail even up to about 5000s duration of the test). The strengthening of these alloys is related mainly with the volume fraction of α phase. Hence, a lower AE level in Mg8Li

alloy in comparison with that in Mg4Li alloy (Fig. 3.2a) is related to the reduction of the amount of α phase which is acoustically more efficient than β phase.

From comparison of AE event rate and the external compressive force during the compression test of pure Mg (99.99%) before (Fig. 3.1a) and after (Fig. 3.1b) single extrusion through angular channel ECAP of square cross section as well as the AE and force behavior in two-phase (α+β)-Mg8Li alloys before and after four-fold ECAP operation, (Figs. 3.4a and 3.4b, respectively), it is possible to conclude that in both cases the level of AE intensity distinctly drops after the ECAP operation, while the analysis of curves of external compressive force indicates to evident increase of plastic properties. The compression tests and AE measurements in the context of ECAP technique allow the statement that reliability of this first pioneer research is to some extent satisfactory. Moreover, the images of microstructures taken before (Fig. 3.4a on the right) and after the ECAP (Fig. 3.4b, on the right) additionally illustrate, that evident refinement of structure takes place after four-fold extrusion through the angular channel, from a few hundred micrometers in the initial state to several micrometers after the ECAP operation. These results are confirmed in next subparagraph 3.2.2, which refers to more detailed and systematic AE measurements in Mg8Li alloys subjected to channel-die compression tests before and after processing in the angular channel but of circular cross section.

A different AE behavior is observed in diphase (α+β)-Mg8Li3Al and Mg8Li5Al alloys (Fig. 3.5a,b, respectively). For example the level of AE activity in Mg8Li3Al (slightly below 10^5/4s≅2.5x10^4/s) is here intermediate between that in Mg (Fig. 3.1) and Mg4Li5Al alloy (Fig. 3.3b). The AE intensity is here at the level of about 2x10^4/s for the Mg8Li3Al alloy while it is much higher in the Mg8Li5Al alloy, i.e. around 3x10^4/s. So, contrary to the single phase alloys, the AE intensity level in the diphase α+β ones increases with the growth of Al concentration. The explanation of such a phenomenon in two-phase alloys is connected with the influence of α+β phase, which generally brings about the increase of their plasticity – as it was mentioned before, the samples do not undergo destruction even up to about 5000s of the compression test duration. It is also bound with the effect of volume fraction of the α phase which is responsible for strengthening of the alloys.

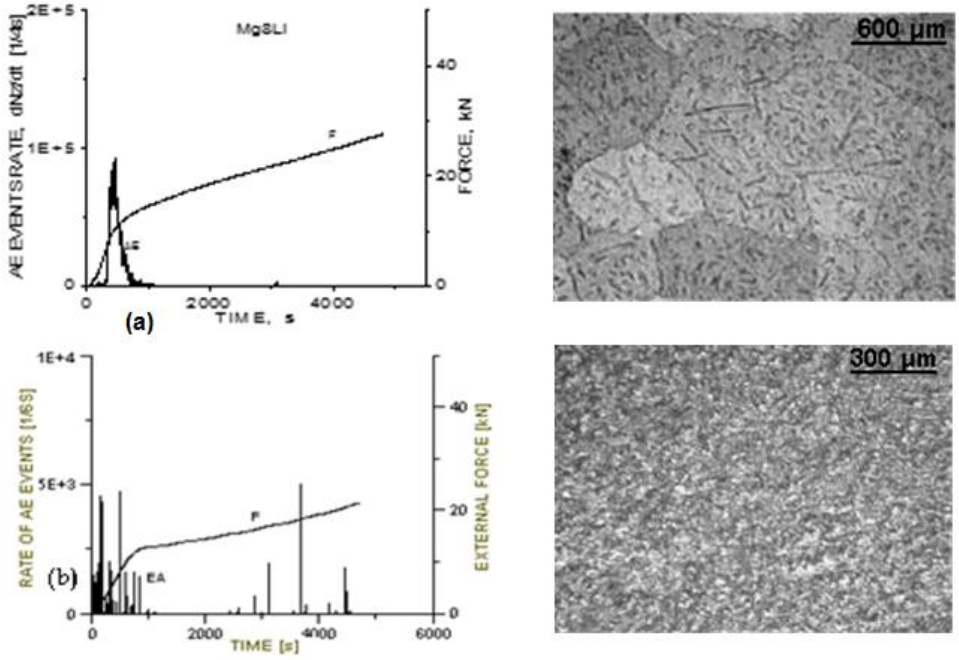

Fig. 3.4. AE and external force in alloys based on two-phase (α+β) matrix subjected to compression at room temperature: (a) - Mg8Li, (b) - Mg8Li after 4-fold ECAP operation. On the right side: relevant images illustrating initial structure of Mg8Li alloy and its refined morphology after 4-fold ECAP operation.

The lower level of AE event rate in pure (α+β)-Mg8Li alloy than that in single-phase α-Mg4Li one is mainly due to distinctly smaller amount of α phase, which is very efficient acoustically. Moreover, it is very interesting, when comparing Fig. 3.2a, Fig. 3.3a and Fig. 3.3b on the one hand and Fig. 3.4a, Fig. 3.5a and Fig. 3.5b on the other hand, one can see that Al addition, in contrary to the case of single α-alloys, does not change essentially the level of AE intensity in diphase (α+β)-alloys, but leads rather to the more jumped-like course of the rate of AE events and the AE activity is observed (though at the considerably lower level) up to the end of the compression test. The effects of Al addition can be discussed on the basis of the strengthening properties of the ternary Mg-Li-Al alloys which generally are related mainly with solid solution hardening caused by Al, the solubility of which is higher in α-Mg-Li than in β phase as well as with the volume fraction of α phase. Though some β phase contribution to the work-hardening may be related with the presence of large (about 2μm) precipitates of LiAl particles, and particularly with their submicroscopic population near phase boundaries α/β [26].

The visible increase of AE with the rise of Al concentration in single-phase Mg4Li based alloys and their growth, although less pronounced, in two-phase Mg8Li ones is due to the rise of Al concentration, which brings about the increase of efficient acoustically volume fraction of α phase [8,26,27], which finds confirmation in relevant microstructures observed in an optical microscope in the state after deformation, in which the α phase is visible as light areas. More details can be found in paragraph 3.2.3 on the example of Mg9Li alloys with different content of Al.

The contribution of β phase to lowering of AE may also come from blocking the movement of dislocations with big LiAl particles. However, a submicron population of LiAl particles (although they occur in the area of interphase boundaries)

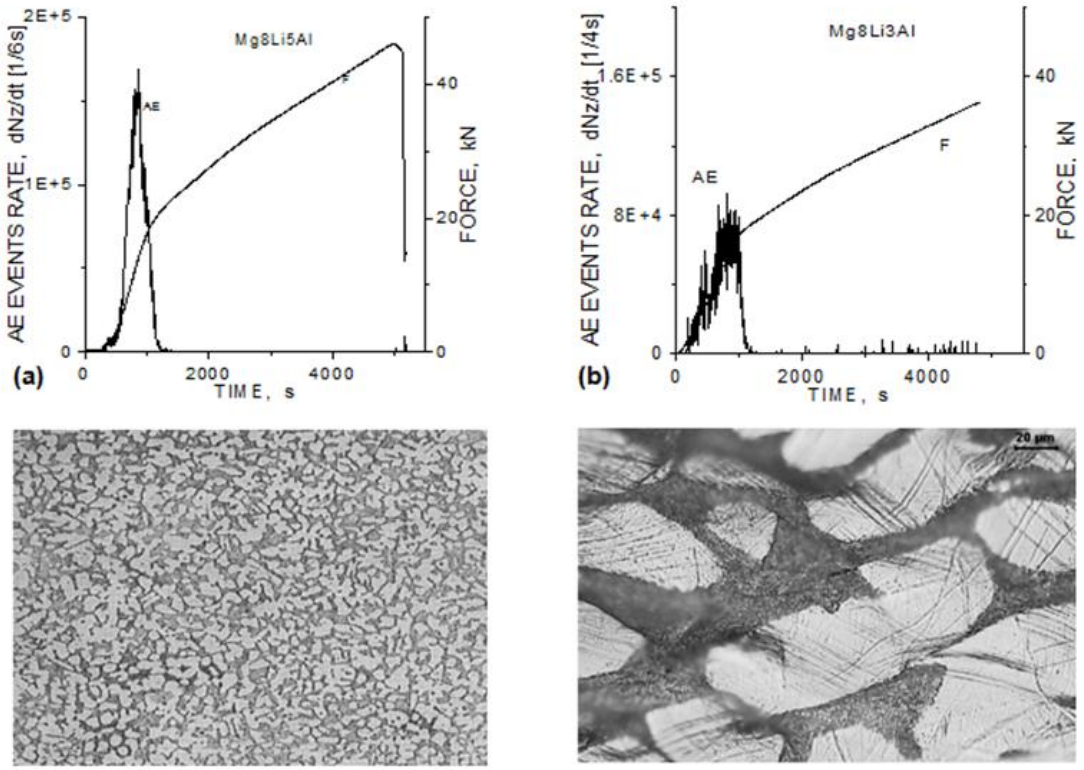

Fig. 3.5. AE in two-phase non-deformed Mg8Li5Al (a) and deformed Mg8Li3Al (b) alloys and their respective typical light microstructures below. Image of Mg8Li3Al is five times magnified than that of Mg8Li5Al.

and coherent $MgLi_2Al$ precipitates, which can also appear in the area of β phase cannot be excluded from being responsible for obstructing the cooperative movement of dislocations [8,26]. In this way a decrease of AE level in Mg8Li3Al for instance is related first to the reduction of the amount of α phase and an increase of β phase which is acoustically not efficient due to the high influence of the lithium diffusivity. Secondly, Al atoms in α solid solution and LiAl particles in β phase being the obstacles for moving dislocations additionally restrict their ability for collective behaviour.

3.2.2 AE in Mg8Li alloys before and after ECAP operations

The investigations of AE in alloys based on Mg8Li matrix have been carried out sporadically and they lacked continuation [4,13,24 and 28,29]. However, a spectacular result was obtained, which was referred to at the beginning of the paragraph (Fig. 3.4). The presented below results were obtained with the use of modified instrument on samples of Mg8Li of different castings and processed in the angular channel ECAP of circular cross-section of dimension 13 mm.

The results of AE investigations in Mg8Li alloy compressed in initial state is shown in Fig. 3.6 whereas compressed after 2- and 4-fold extrusion through angular channel of circular cross-section at temperature 100°C are shown in Figs. 3.7 and 3.8, respectively. Processing at 100°C was imposed, among others, by the problem of choice of processing conditions for composites in the ECAP channel.

The optical images of microstructures after respective ECAP operations taken of two sample areas: at the side and in the middle are presented in each further figures in their central part. Moreover, in order to assess the refinement degree of structure, TEM microstructures are placed below, which together with respective light images illustrate the structure refinement of Mg8Li alloy after ECAP performed at 100°C.

Analyzing Figs. 3.6-3.8 it can be stated, that the number of AE events, according to anticipation, distinctly decreases with the elevation of numbers of ECAP operations, so that after 4 runs, a constant, low level was achieved, which was comparative with the background originated from noises of the instrument.

The light images of microstructure, in fact, reflect the refinement of structure not too well, so TEM observations were carried out, but they disclose the fact, that the refinement is not homogeneous in the whole area of the sample. It can be seen, that the refinement in the middle part of the specimen is more homogeneous than in the area close to the edge.

TEM microstructures successively show proceeding refinement of the structure, so that after already 4 ECAP operations, the size of crystalline areas is few hundred nanometers, often even below 500 nm (Fig. 3.8, TEM microstructure below, on the right). The obtained

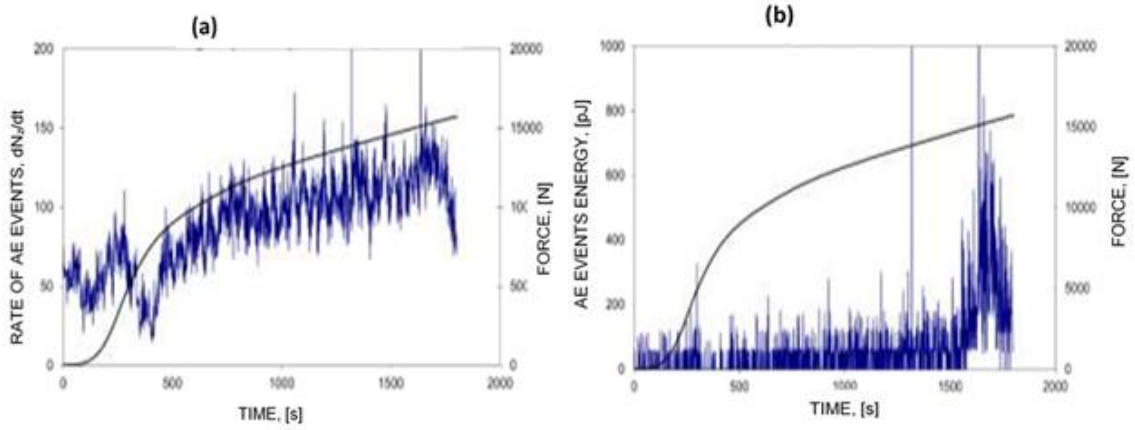

Fig. 3.6. AE parameters: number of events (a) and energy of events (b) in Mg8Li alloys externally loaded, compressed before ECAP.

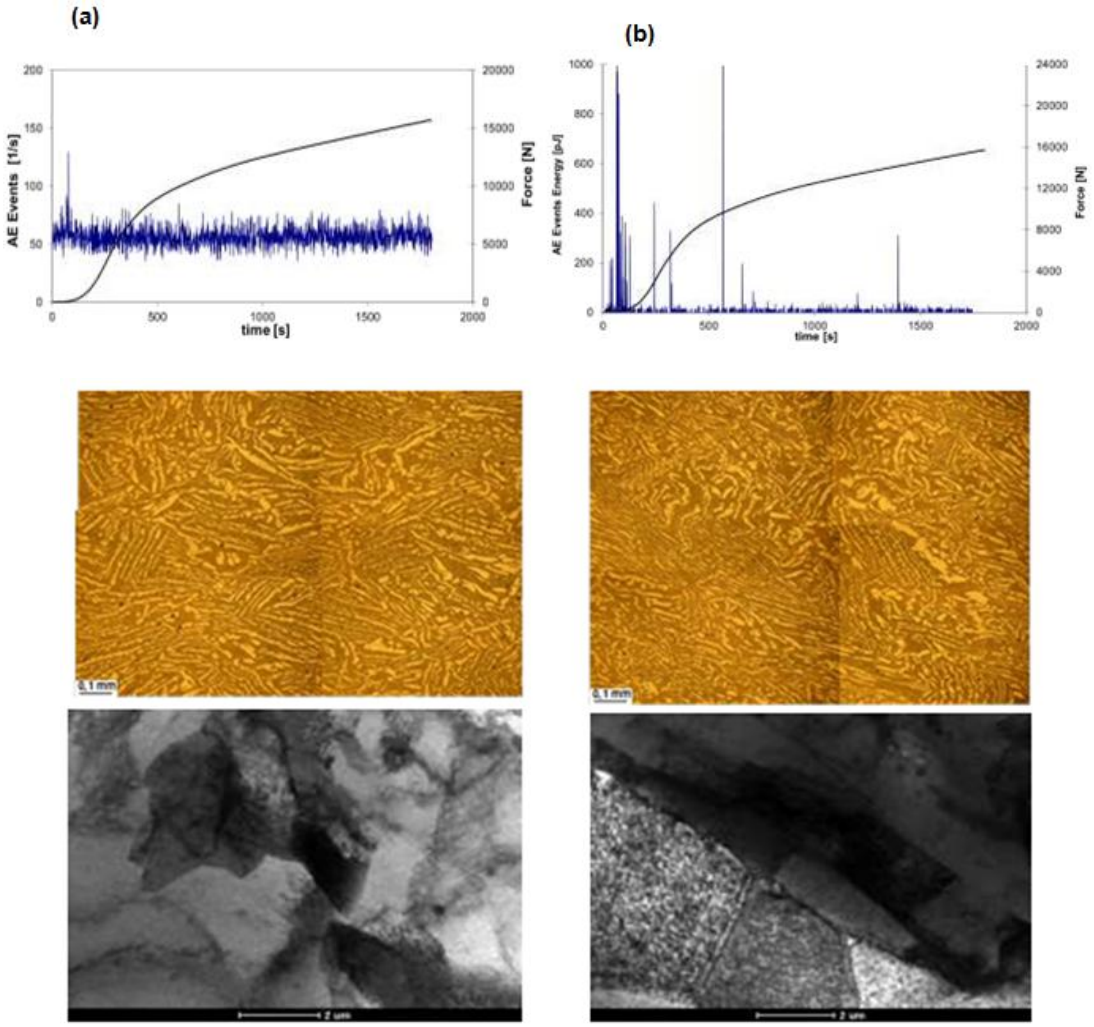

Fig. 3.7. Courses of external force and AE parameters: number of events (a) and energy of events (b) in Mg8Li alloys compressed after 2-fold processing in the ECAP channel at temperature 100°C. Optical and TEM microstructures in the middle and at the bottom, respectively.

structure can be qualified somewhere between ultrafine-grained and almost nanocrystalline. It needs to be added, that the electron diffractions (SAEDP) may confirm the greater effect of refinement through blurring the reflections (Fig. 3.9 on the right) from the material after 4th ECAP compared with the reflections in Fig. 3.9 (on the left) of 2-fold one.

3.2.3 Mg9Li, Mg9Li1Al, Mg9Li3Al and Mg9Li5Al alloys

The compression tests of series of Mg9Li, Mg9Li1Al, Mg9Li3Al and Mg9Li5Al alloys were performed before and after heavy deformation of HPT type. They were particularly systematic because the tests were carried out for samples subjected to one- to four- and 6-fold HPT processing. The optical and TEM observations followed in order to make things more complete. Fig. 3.10 presents initial microstructures of the new series of Mg9Li (Fig. 3.10a), Mg9Li1Al (Fig. 3.10b) and Mg9Li3Al (Fig. 3.10c) as well as Mg9Li5Al (Fig. 3.10d).

It can be clearly seen that the volume fraction of hexagonal α phase increases with the growth of alloying addition of Al, which manifest themselves as light regions in the background of dark places of β phase of cubic structure. These observations strongly confirm the fact, that the AE increase with the rise of Al content – what is

distinctly seen in Figs. 3.12a to 3.14a – is the result of elevated volume contribution of α phase acoustically very efficient.

Figs. 3.11-3.14 collect the results of AE behavior in the Mg9Li alloys (Fig. 3.11) and Mg9Li5Al (Fig. 3.14) subjected to compression tests before and after one, two, four and six HPT runs as well as in Mg9Li1Al (Fig. 3.12) and Mg9Li3Al (Fig. 3.13) alloys compressed before and after one and three runs using HTP technique. Furthermore, respective microstructures of Mg9Li alloy in the initial state in Fig. 3.11b and 6 times processed with HPT (Fig. 3.11g) are included. Also the microstructures of Mg9Li1Al alloys after 3-fold HPT processing (Fig. 3.12d) are here enclosed. These TEM images illustrate the degree of refinement obtained with the use of HPT technique.

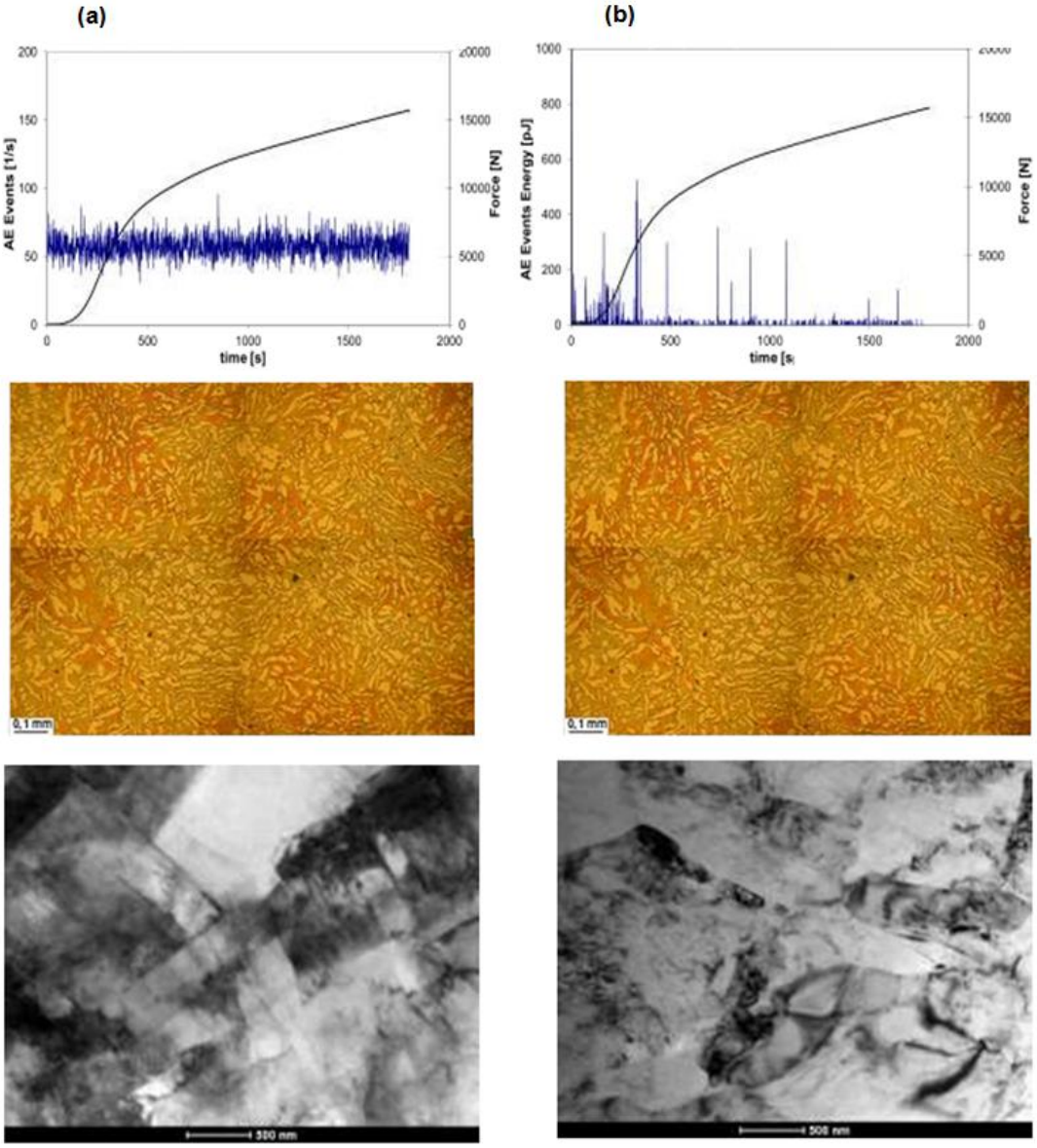

Fig. 3.8. Runs of external force and AE parameters: number of events (a) and energy of events (b) in Mg8Li alloys compressed after 4-fold processing in the ECAP channel at 100°C. Optical microstructures in the middle and TEM images below.

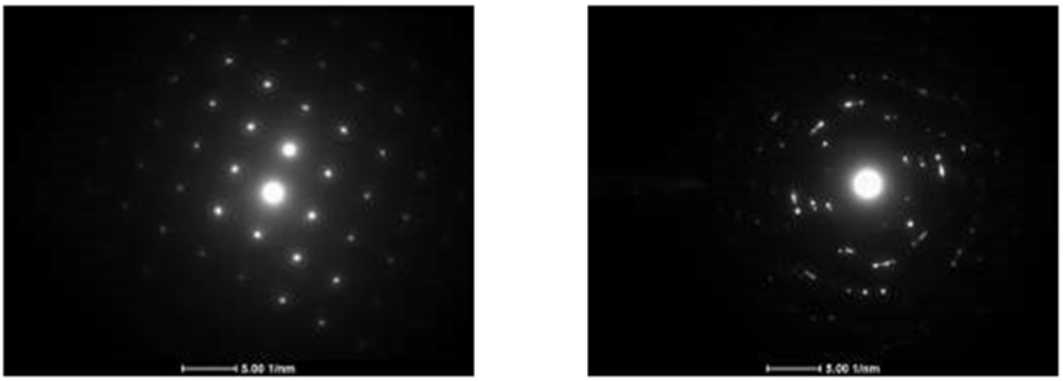

Fig. 3.9. Diffractions of Mg8Li alloy processed in ECAP twice (left side) and four times (right).

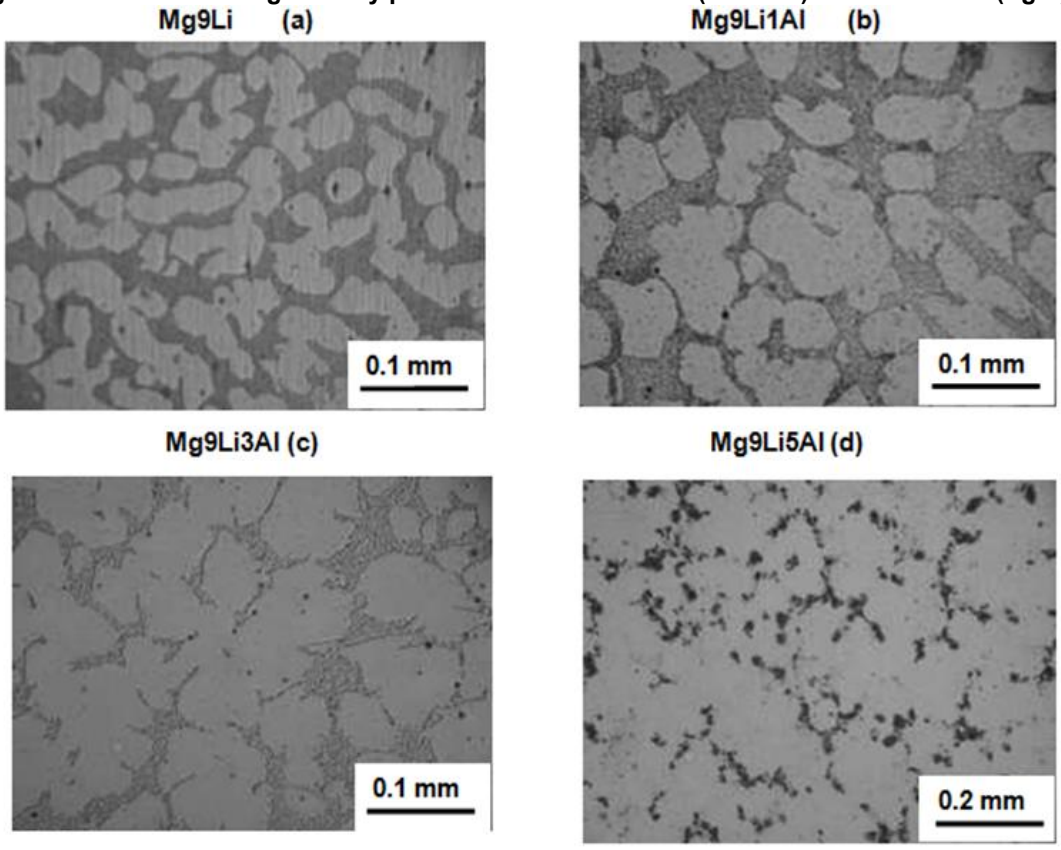

Fig. 3.10. Microstructures of new series of alloys based on Mg9Li matrix obtained using optical microscopy: (a) – Mg9Li, (b) – Mg9Li1Al, (c) – Mg9Li3Al, (d) – Mg9Li5Al.

Fig. 3.11a illustrates the changes of AE parameter in the form of event rate and compressive force in function of time for the Mg9Li alloy in the initial state, i.e. before the use of HPT. Figs. 3.13b and 3.13c present these dependencies after first and three-fold HPT processing, while Figs. 3.11e and 3.11f after fourth and six-fold use of HPT. Analogous description refers to Mg9Li5Al alloy (Fig. 3.14), while Fig. 3.12a shows the AE behavior and compressive force of Mg9Li1Al before HPT and Figs. 3.12b and 3.12c the same dependencies after single and three-fold HPT operations. An analogous description refers to Mg9Li3Al alloy sample (Fig. 3.13).

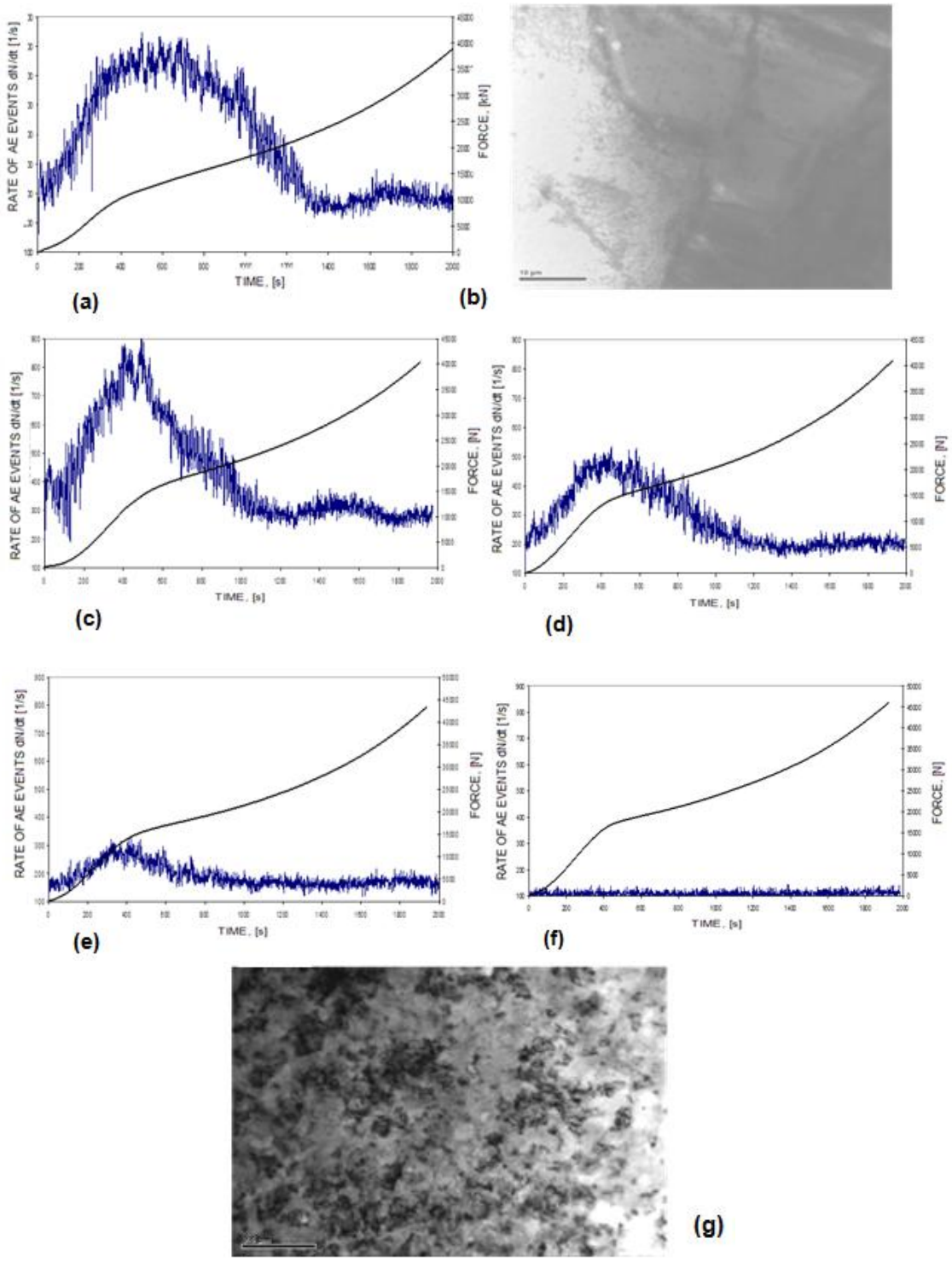

Fig. 3.11. Changes of AE and compressive force in Mg9Li subjected to compression tests before (a) and after single (c), two-fold (d) as well as after 4-fold (e) and 6-fold (f) HPT operation; (b) - TEM image of microstructure of Mg9Li alloy prior to and (g) after 6-fold HPT.

Furthermore in Fig. 3.15 the changes of AE and compressive force are presented for the samples of Mg9Li1Al, Mg9Li3Al and Mg9Li5Al alloys in the form of cubes of 10 mm side. It should be

explained that the dependences of AE and force on time shown in Figs. 3.11a, 3.12a and 3.13a as well as 3.14a differ quite essentially from the results of Fig. 3.15 because the samples of Figs. 3.11-3.14 were in the form of discs 10 mm in diameter and 2-3 mm of thickness, so the results for those samples were referential to those processed with HPT method.

In result, analyzing and comparing the behavior of AE in the samples of compressed alloys before (e.g. Figs. 3.11a and 3.14a) and after the application of the HPT method (Figs. 3.11c, d, e, f and 3.14b, c, d, e) it can be concluded that the intensity level of AE, measured with the average value of number of AE event recorded evidently decreases with the growth of multiplication factor of HPT operation for the specimens processed with the HPT technique in relation to unprocessed material. It should be noticed, that for the samples processed 6 times (Figs. 3.11f and 3.14e) the AE practically decays, which is well visible in the case of the Mg9Li alloy (Fig. 3.11f), where the background prevails due to the noise from the instrument.

3.2.4 Verification of new series of Mg9Li based alloys tested with the use of new HPT instrument

Mg9Li alloys. Observations of Mg9Li alloys in light and TEM microscopes showed that, firstly, the AE increase with the increase of Al content results from greater volume contribution of α phase, which is very efficient acoustically, and secondly, that the level of intensity and AE activity degree evidently drops with the growth of multiplication factor of HPT operations, which is the effect of refinement of structure confirmed with TEM.

It is important, that in the case of the old HPT device, described in former subparagraph 3.2.3, the samples were prepared in the form of disks of diameter 10 mm, while the new one imposed the diameter of 13 mm. Then the samples predicted for further compression tests in the angular channel had to be cut in such a way, that the resulting plates were in the form of squares with side 10 mm. The verifying studies of AE were performed for new series of castings of

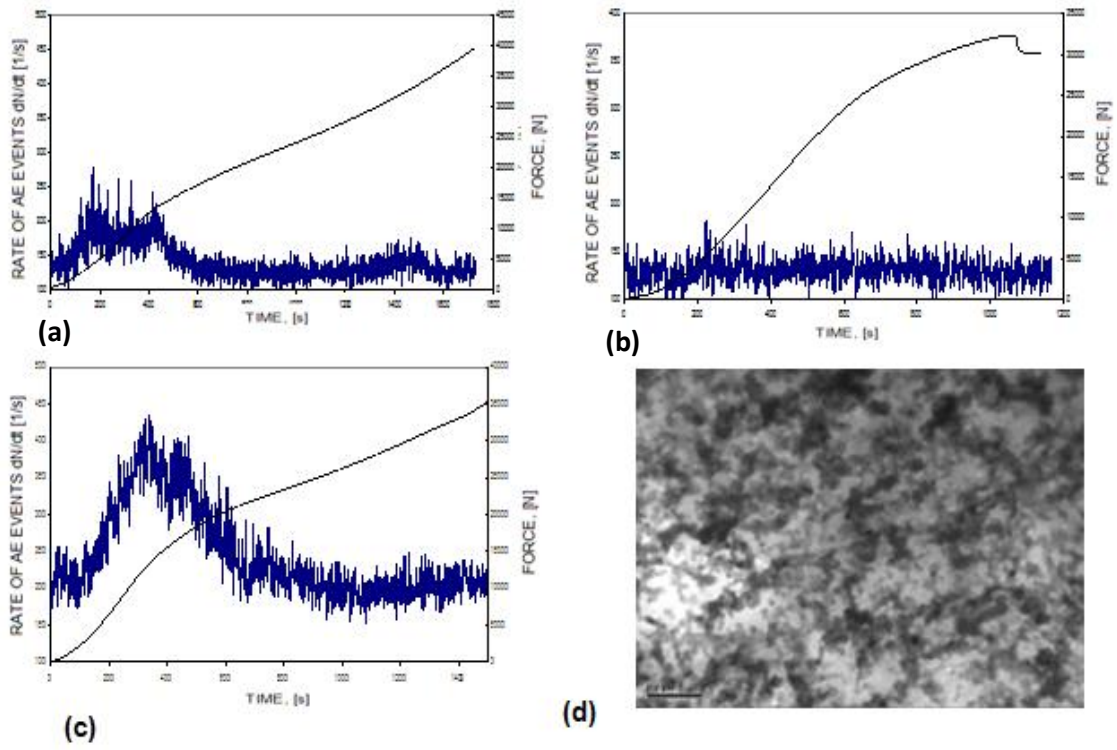

Fig. 3.12. Recordings of AE and compressive force of Mg9Li1Al alloy compressed before (a) and after single (b) and three-fold (c) HPT operation; (d) - TEM macrostructure of the alloy three times treated with HPT.

Mg9Li, Mg9Li1Al and Mg9Li5Al to see whether the conclusions from earlier studies are universal and do not depend on HPT device and the form of samples for compression tests.

Moreover, in the study described here, an updated software in the form of new card of ADLINK type was applied for the spectral analysis of AE signals, which enabled the increase of the instrument sensitivity by order of magnitude. At the same time, apart from the conventional recordings of numbers of AE events, diagrams of event energy in function of compression time were obtained.

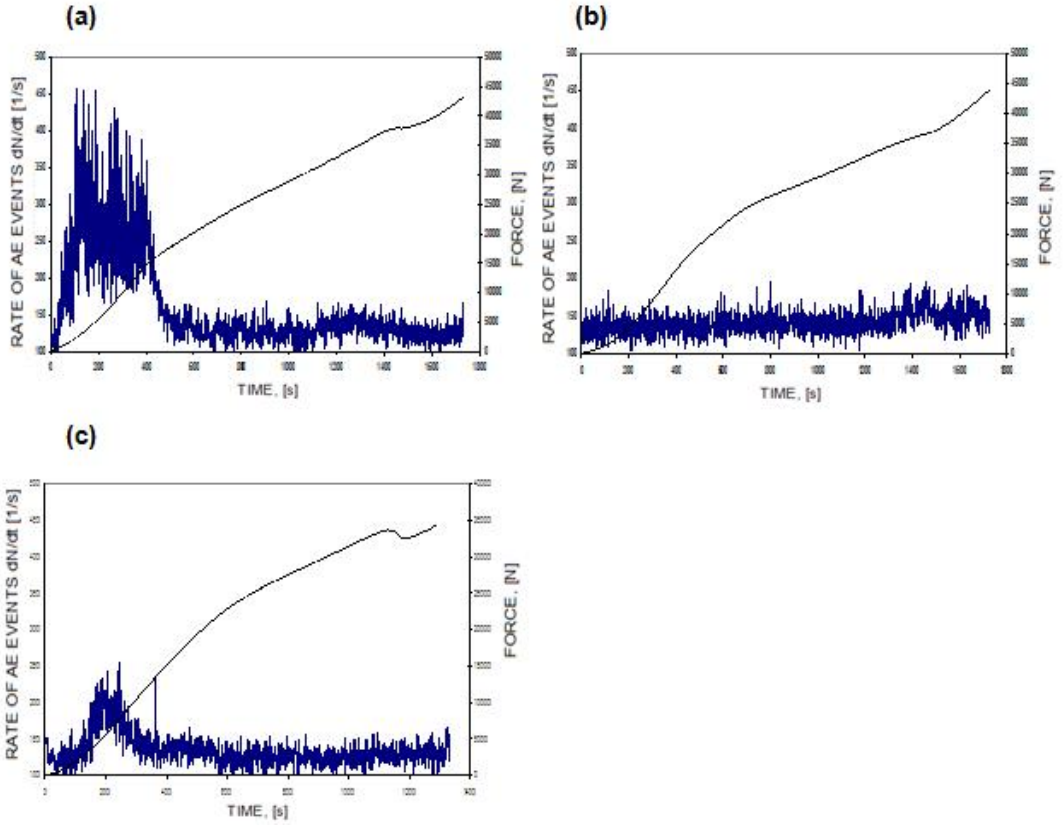

Fig. 3.13. Changes of AE and compressive force in Mg9Li3Al subjected to compression tests before (a) and after single (b) and three-fold (c) HPT operation.

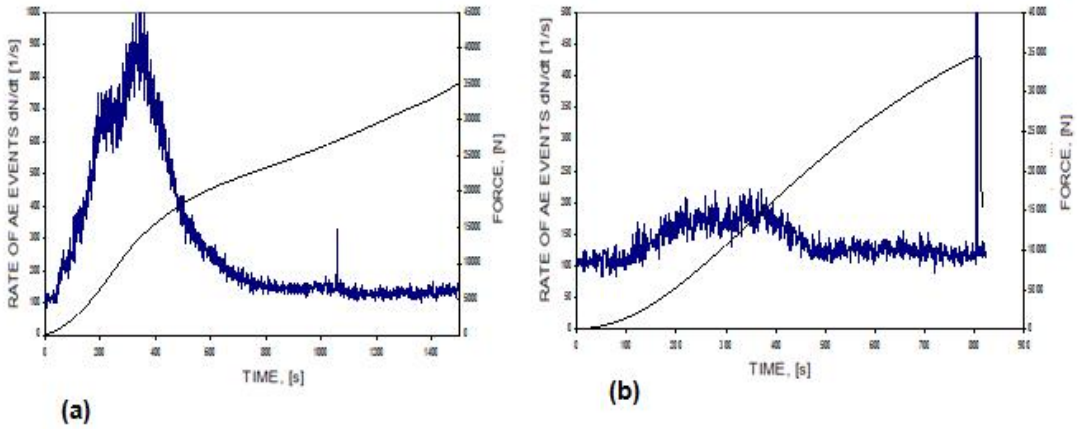

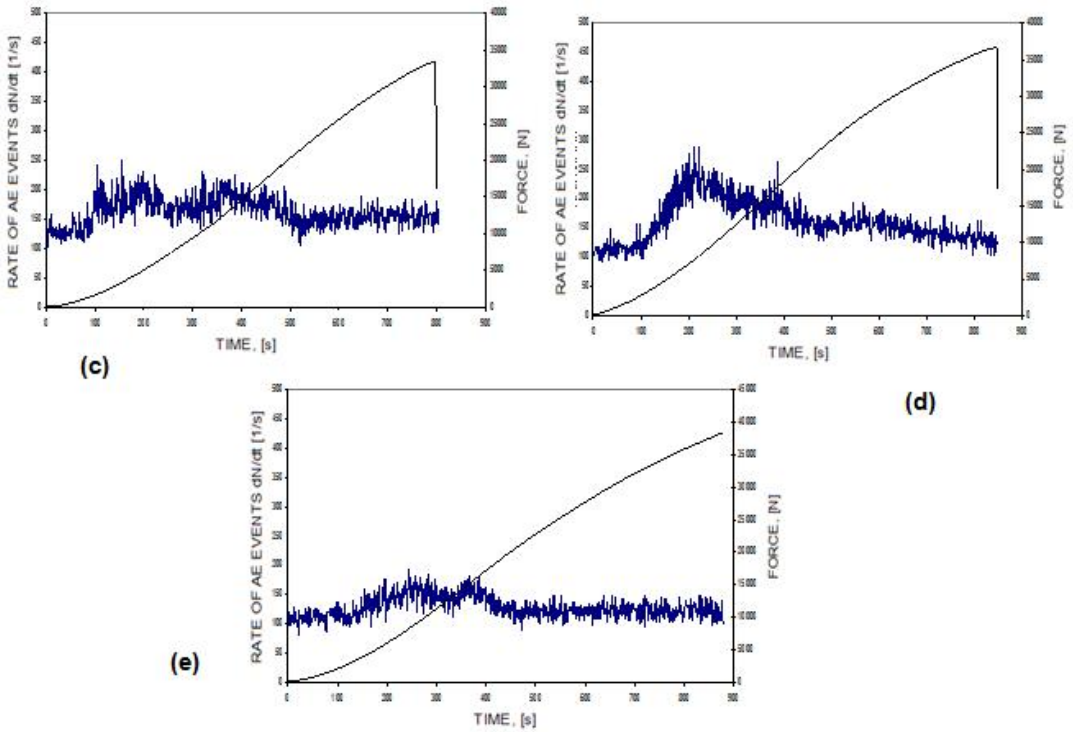

Fig. 3.14. AE and compressive force of Mg9Li5Al alloy subjected to compression tests before (a), after single (b), two-fold (c) and four-fold (d) as well as 6-fold HPT (e) processing.

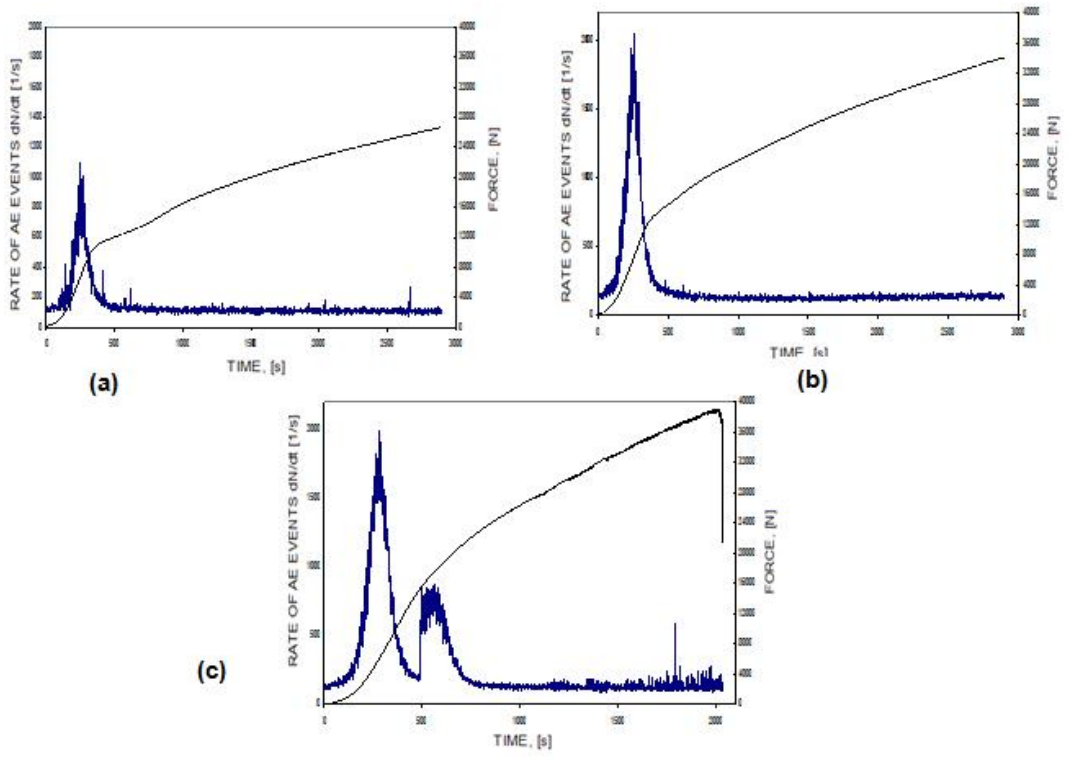

Fig. 3.15. AE and compressive force in cubic samples of Mg9Li1Al (a), Mg9Li3Al (b) and Mg9Li5Al (c) alloys subjected to compression tests.

The changes of AE event number, its energy and external force against compression time of Mg9Li alloy in its initial state are presented in Figs. 3.16a and b, respectively together with TEM microstructure below. Accordingly, the behavior of AE in the alloy processed with HPT is placed in Figs. 3.17a, b, c, and d after one and three runs, respectively, followed with appropriate TEM images.

In turn, in Figs. 3.18a and b the changes of load and energy of AE events are shown for Mg9Li alloys compressed after 5 and 6 HPT operations, respectively. The TEM images shown in the middle illustrate the degree of microstructure refinement, confirmed by diffraction patterns recorded after one and six HPT runs. Based on Figs. 3.16-3.18, it can be stated that the effect of AE event drop is clearly visible only after three-fold HPT rotation (Fig. 3.17). Next rotations do not basically change anything. The same refers to the structure refinement, which is confirmed by blurring of reflections in the diffraction patterns after 6-fold HPT (Fig. 3.18 at the bottom on the right) compared with more or less sharp reflections after a single HPT processing (at the bottom, on the left).

Mg9Li1Al alloys. Similarly to earlier schedule, the behavior of AE and microstructures, for example after 4- and 6-fold processing with the use of HPT technique, are shown in Fig. 3.19, in which as points of reference, courses and AE event numbers as well as its event energy (Figs. 3.19a and b) for the initial state are presented, respectively, while in Figs. 3.19c and d, changes of AE event energy after four and six HPT rotations are shown together with microstructures in the initial state and processed 6 times below.

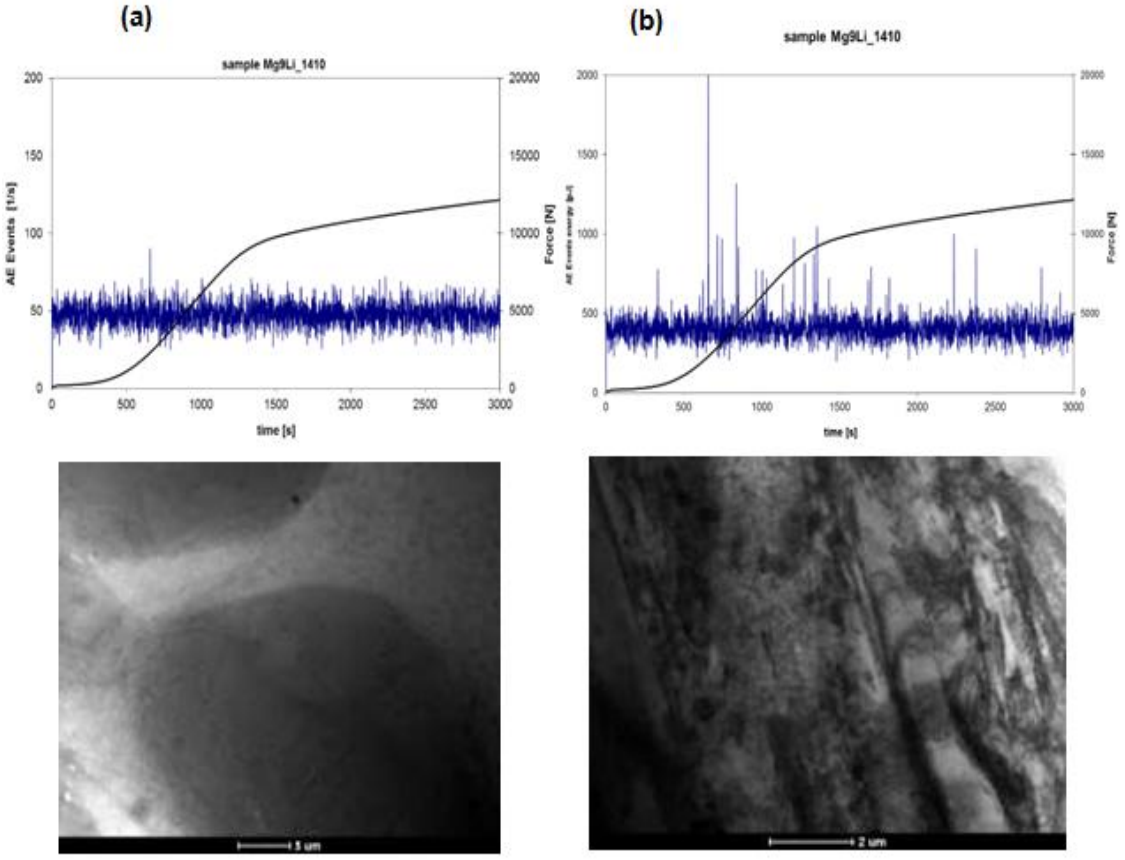

Fig. 3.16. Courses of external force and AE event number (a) and event energy (b) in Mg9Li alloy compressed prior to HPT operation. TEM microstructures in various magnifications below.

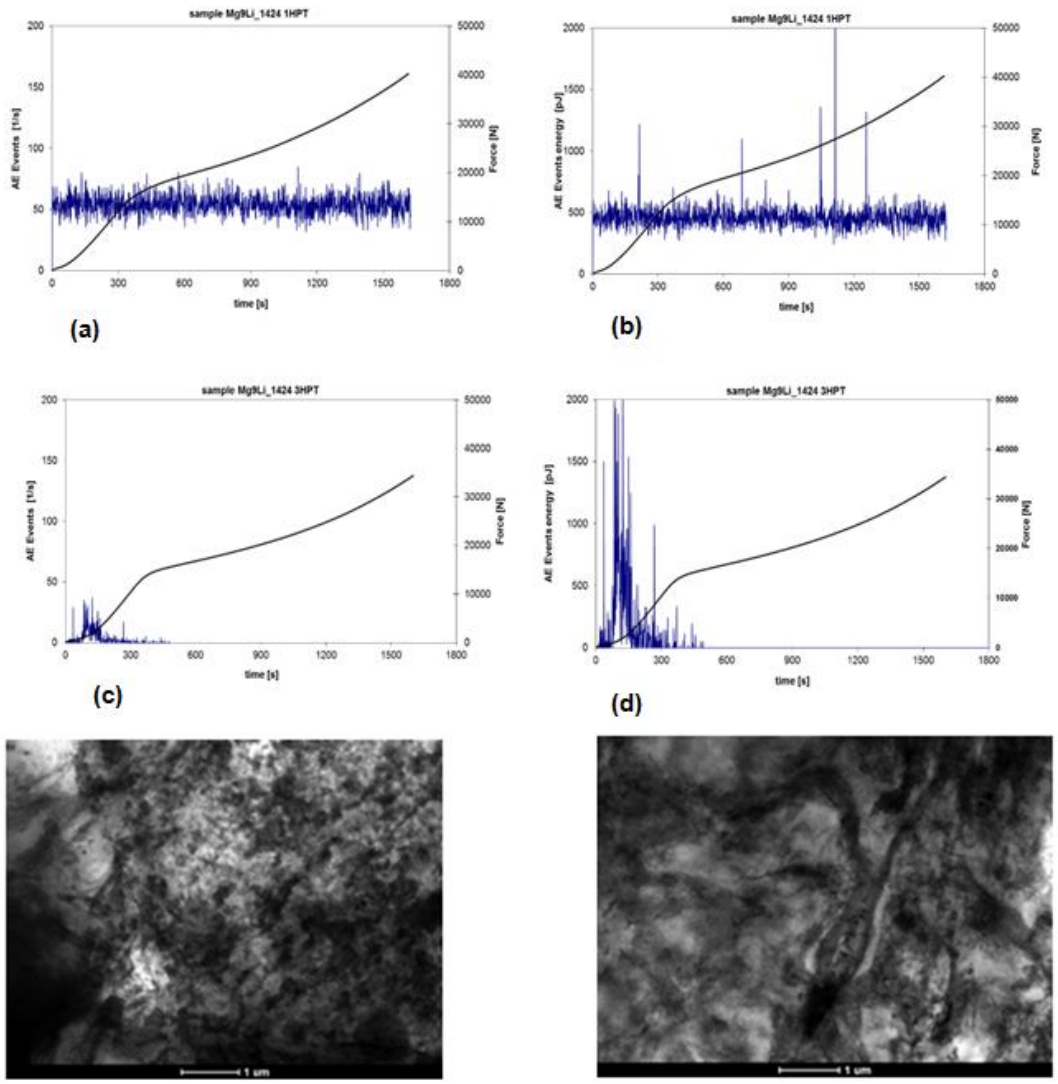

Fig. 3.17 Courses of external force and AE event number (a) and event energy (b) in Mg9Li alloy compressed after one HPT processing and changes of external force and AE event number (c) and event energy (d) in this alloy compressed after three HPT runs together with its TEM images after HPT processed once (on the left) and trice (on the right).

A distinct increase of strength is also visible in the Mg9Li1Al alloy, particularly after 6-fold HPT (at max. load 45kN) accompanied by a significant decrease of AE followed by structure refinement.

Mg9Li5Al alloys. Their AE behavior in the context of strength properties and microstructure were at random examined prior to and after 3- and 6-fold HPT processing. The obtained results are inserted in Fig. 3.20, in which, as reference, courses of AE event number and event energy together with appropriate TEM microstructure for the initial state are presented, while in Fig. 3.21 the plots refer to the specimens compressed 3 and 6 times with HPT. It yields from the analysis of both figures, that a visible improvement of strength: maximal force after 3-fold HPT is of order 60kN, compared with a little more than 20kN for the initial state. Such a big increase of strength results from the refinement of structure, according to Hall-Peach relationship, which - as it is believed – refers also for ultrafine-grained materials of grain size from several to a dozen or so micrometers, but not necessarily to nanocrystalline structures of few hundred

nanometer-grain size. The structure refinement is accompanied with the decrease of AE intensity and activity, which is visible already after 3-fold HPT operation due to the deformation strengthening of material connected with the increase of dislocation density, which obstruct the collective behavior of groups of new dislocations generated from sources and subjecting to internal and surface annihilation. These factors, in the author's opinion, contribute quite a lot to the recorded AE signals. Moreover, after 3- and 6-fold rotations, the number as well as AE event energy reach their lowest level only a little higher than the average level of instrument noise background.

Comparing the initial stages in Figs. 3.16a,b, 3.19a,b and 3.20a,b for Mg9Li, Mg9Li1Al and Mg9li5Al alloys, respectively, one can assess the influence of Al on AE. The level of AE event number visibly increases for the alloy with 1% Al, although it remains constant for the sample with 5% Al and it is difficult to say why it is like that. However, on the other hand, the level of AE event energy is visibly higher in the case of 5% Al than in case of 3% Al content.

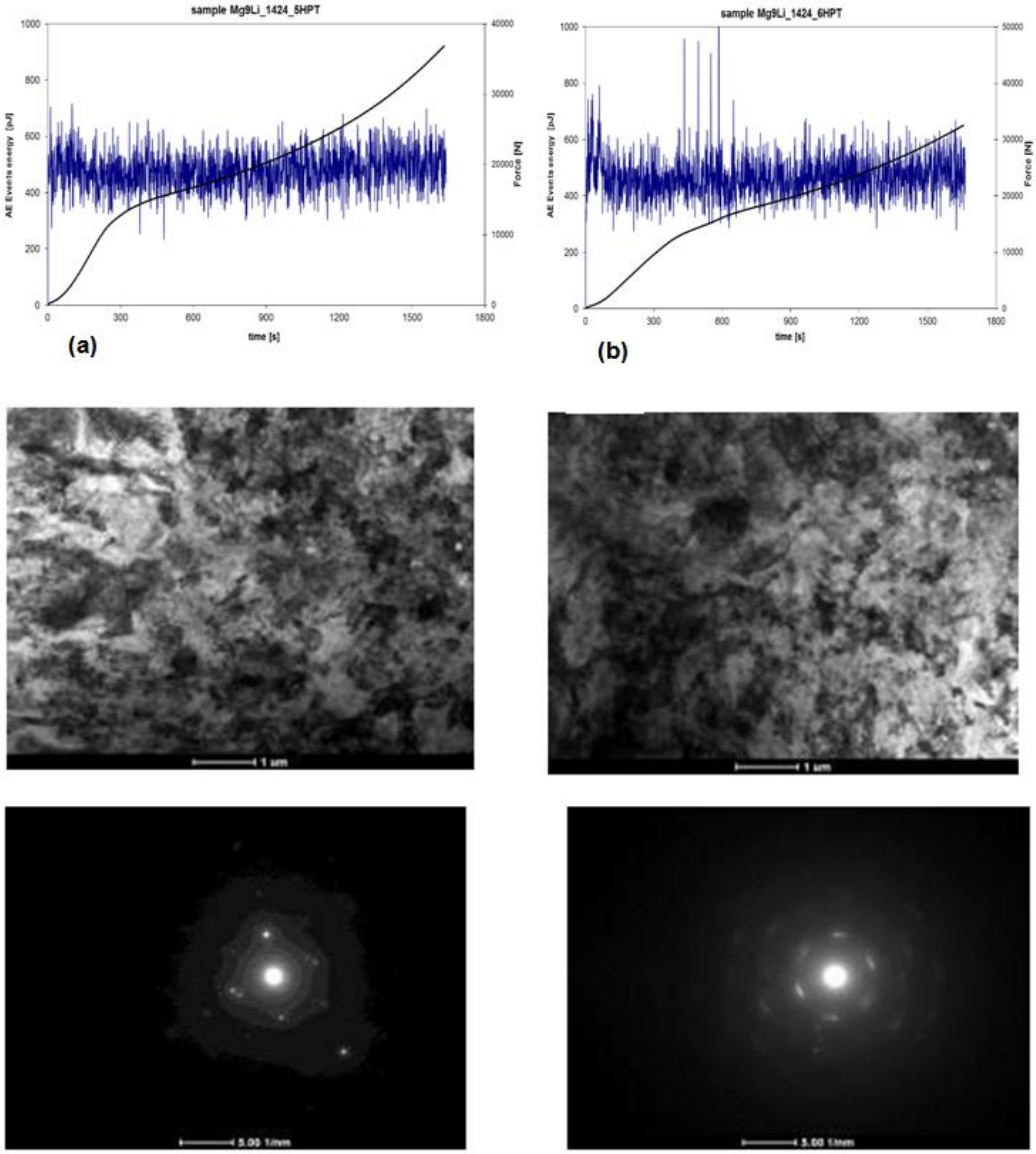

Fig. 3.18. Courses of load, AE event energy (a, b) and TEM microstructures (in the middle) in Mg9Li alloy HPT processed 5 (left) and 6 times (right). Below respective diffraction patterns.

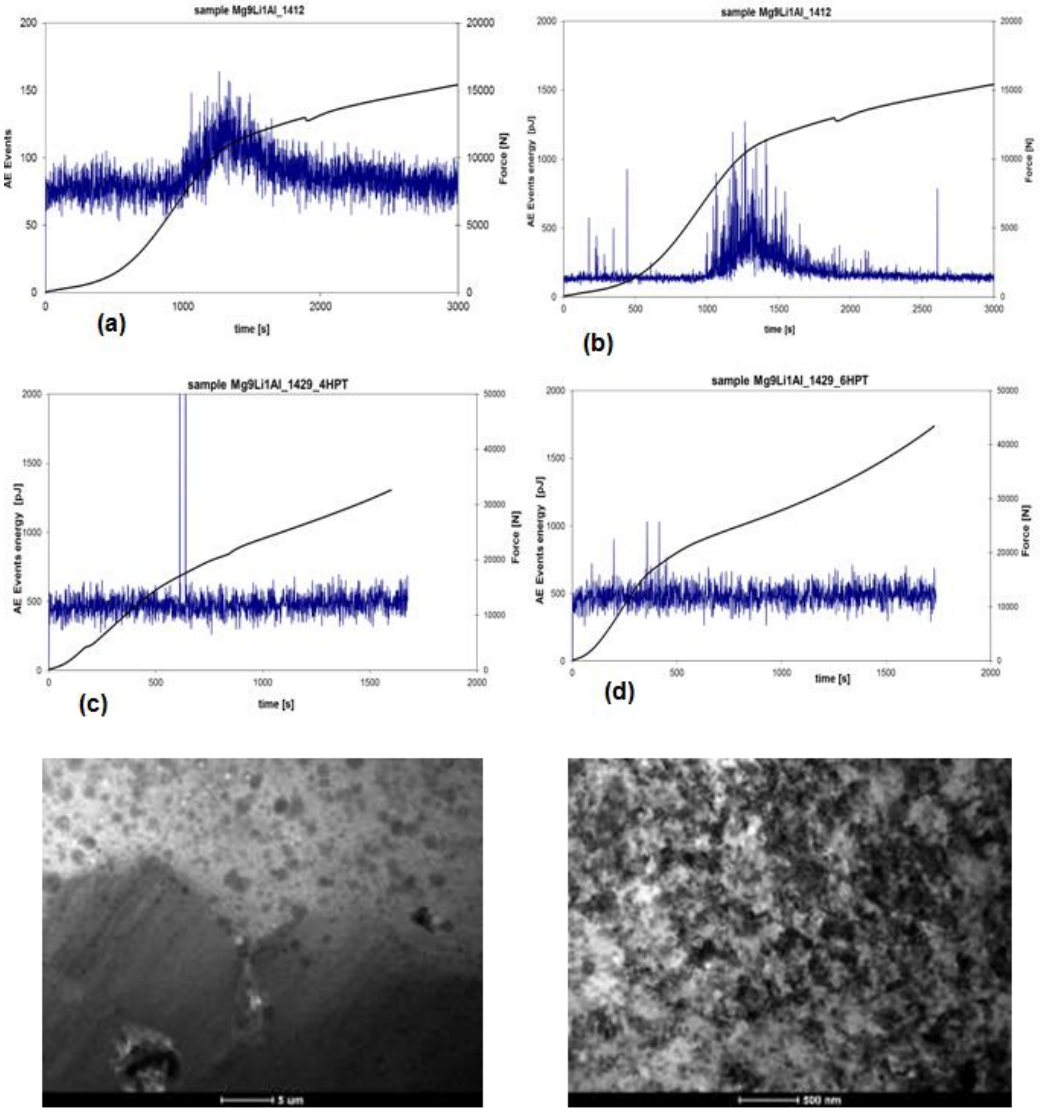

Fig. 3.19. Changes of AE event number and energy on the background of load of Mg9Li1Al alloy compressed prior (a, b) and event energy after 4- and 6-fold HPT operations (c, d), respectively.
Below: TEM microstructures – initial on the left and 6-fold processed on the right.

Furthermore, one needs to keep in mind, that in this above discussed case as well as in other cases of unexpected AE recordings, they may be affected by such factors as different casting, inhomogeneity and different shape of samples and varying chemical composition as well as different HPT instrument, not to mention about repeatability of measurements. A few, let's say minimum up to three measurements for the same type of samples often go beyond the time and technical frame of the experiment. But courses of AE energy and events rather fulfill the expectations of researcher, because the maximum values of energy of individual AE signals visibly increase for the Mg9Li5Al alloy (Fig. 3.20b) compared with Mg9Li (Fig. 3.16b) and Mg9Li1Al sample (Fig. 3.19b). The observation also suggests, that the α phase in two-phase alloys based on Mg9Li matrix is not only more efficient acoustically than the β phase, but also it generates AE impulses which are greater, the higher is Al content under the same order of load.

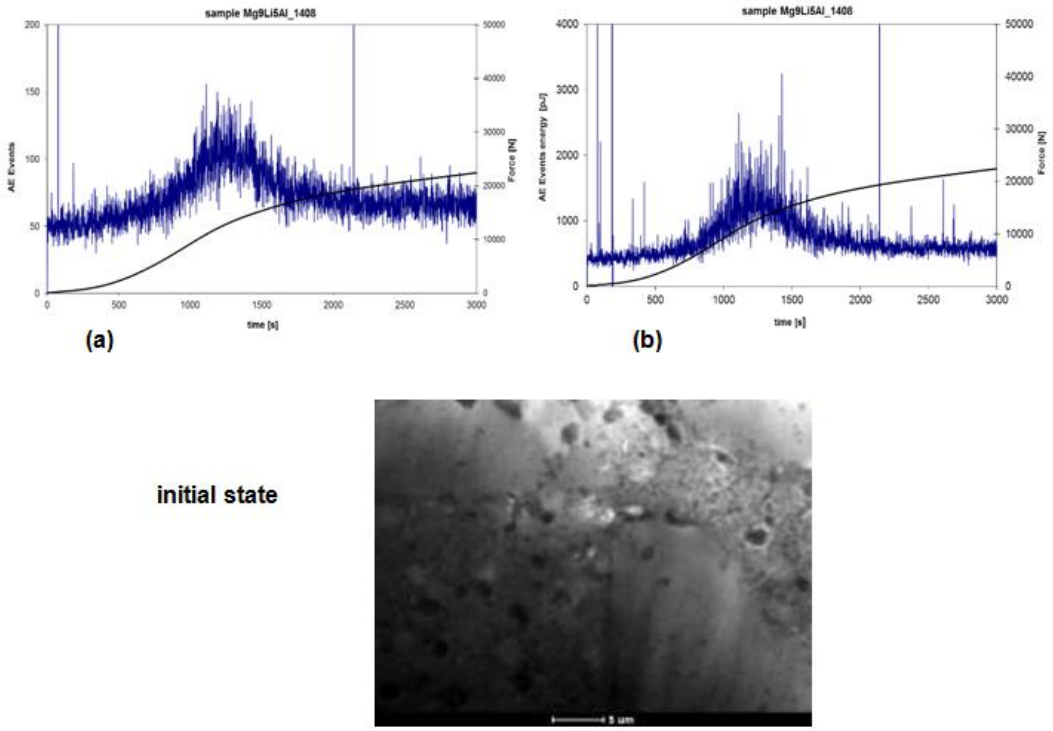

Fig. 3.20. Number of AE events (a) and energy (b) on the background of load of Mg9Li5Al alloys before HPT operation.
Below, respective TEM microstructure in the initial state.

It should be still added, that apart from strengthening of material, the reason for the decrease of intensity and activity of AE with the increase of number of HPT operations may be another mechanism, e.g. slip along grain boundaries, as in the case of superplastic deformation. Such mechanism can come into action in ultra-fine grained materials as it suggest in our earlier works [4,24,30-32]. So, as seen, that it is reasonable to think, that the slip mechanism along grain boundaries – which has not been satisfactorily acknowledged so far – generates AE to a much lesser extent than well understood dislocation mechanism of slip inside the grains. A verification of the hypothesis should require however systematic and much more detailed examinations focused on one precisely selected material and precise analysis of individual AE signals.

3.2.5 Mg10Li, Mg10Li1Al and Mg10Li5Al alloys

Alloys based on Mg10Li. Figs. 3.22-3.24 show results of AE behavior obtained for a new series of Mg10Li, Mg10Li1Al, Mg10Li3Al and Mg10Li5Al alloys, which were subjected to channel compression tests prior and after processing with the method of intensive deformation of HPT type. The AE behavior in Fig.3.22 is presented in the form of parameter of event rate for the Mg10Li alloy before (a) and after 3-fold HPT (b). TEM image (c) illustrates degree of microstructure refinement due to HPT processing. The series of examination ends up with the results for the Mg10Li5Al alloy (Fig. 3.23), in which the AE event rate and compressive force are shown prior to (a) and after 3-fold working with the HPT method (b). It was established, similarly to the reference alloy, that 3-fold HPT processing resulted in the grain refinement, visible in TEM image (c).

Eventually, the series of the examinations was summarized with summary plot of AE event energy distribution registered for each alloy before and after HPT processing. The distributions reflect, first of all, how high the energy corresponding to maximal number of AE events is (in conventional units). Analysis of the above results allows establishing, that its maximum values correspond to alloys with Al content, which were processed twice or trice with HPT. According to Fig. 3.24, it corresponds to

values about 400, 450 and 600 units for alloys denoted as Mg10Li3Al 2HPT, Mg10Li5Al 3HPT and Mg10Li1Al 2HPT. In turn, in can be noticed, that except from the Mg10Li1Al alloy after 3xHPT, all three lowest values of the energy correspond to that of their initial states, i.e. subjected to compression test before the application of HPT technique.

As a result, by analyzing and comparing the behavior of the EA in the samples before (Fig. 3.25a) and after the HPT processing (Fig. 3.25b), respectively, it can be said that the level of intensity of the EA measured with the average value of registered number of its events clearly decreases for the samples processed with HPT in relation to unprocessed ones, while, at the same time, the energy corresponding to the highest number of AE events increases, as was observed earlier based on analysis of diagrams of Fig. 3.24.

In order to make things complete, the results for the Mg10Li1Al alloy before and after 3-fold HPT processing are presented in Fig. 3.25a, b, respectively. It was stated that the diagrams of AE for the Mg10Li3Al alloy recorded before and after HPT processing run in a quite similar way to these obtained for Mg10Li3Al sample, so they are not included.

3.3 AE in Single β Phase Alloys of *cubic* Matrix

3.3.1 Mg12Li, Mg12Li3Al and Mg12Li5Al

According to the courses of AE events presented in previous chapters, the AE behavior in single β-Mg12Li alloys shown in Fig. 3.26a is extraordinarily different from so far discussed events and from the point of view of physical reasons it is by no means interesting, because the level of AE intensity is very low.

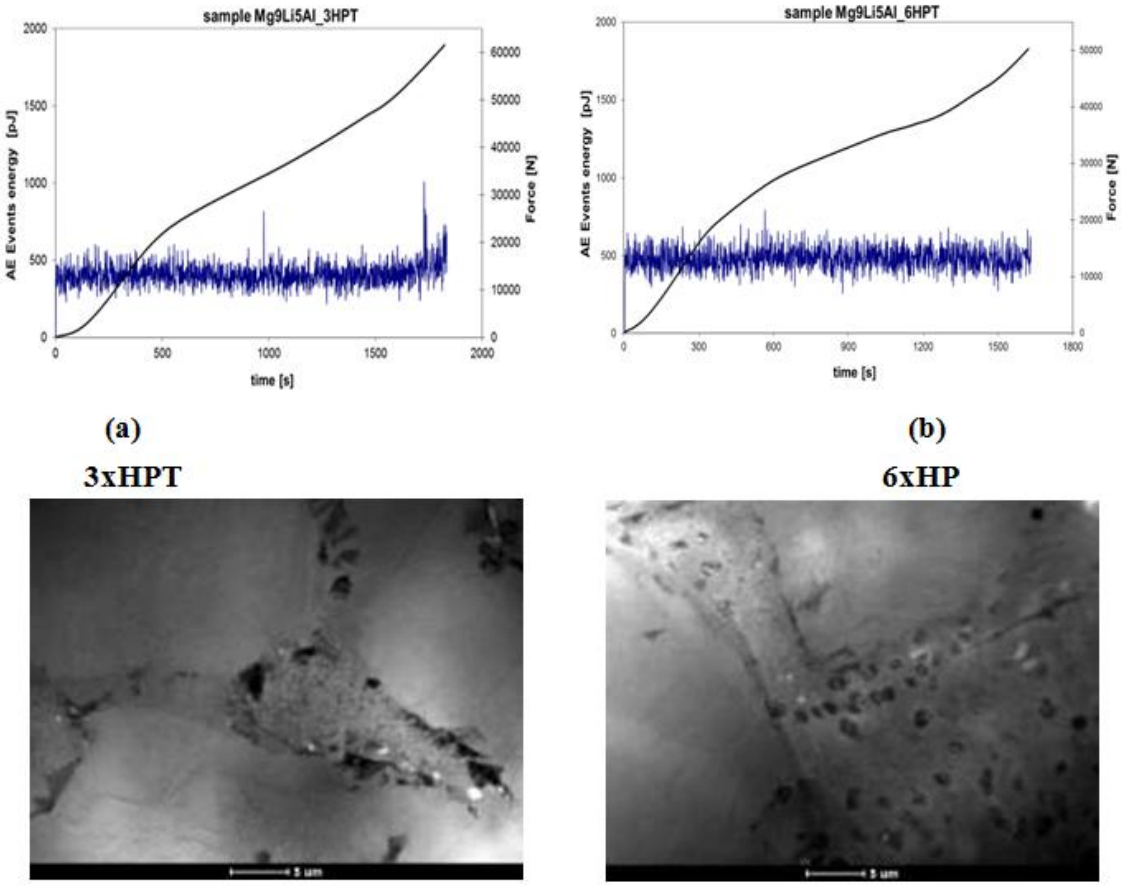

Fig. 3.21. Plots of external load and AE event energy in Mg9Li1Al alloy compressed after 3 (a) and 6 (b) HPT rotations. Below respective microstructures after HPT.

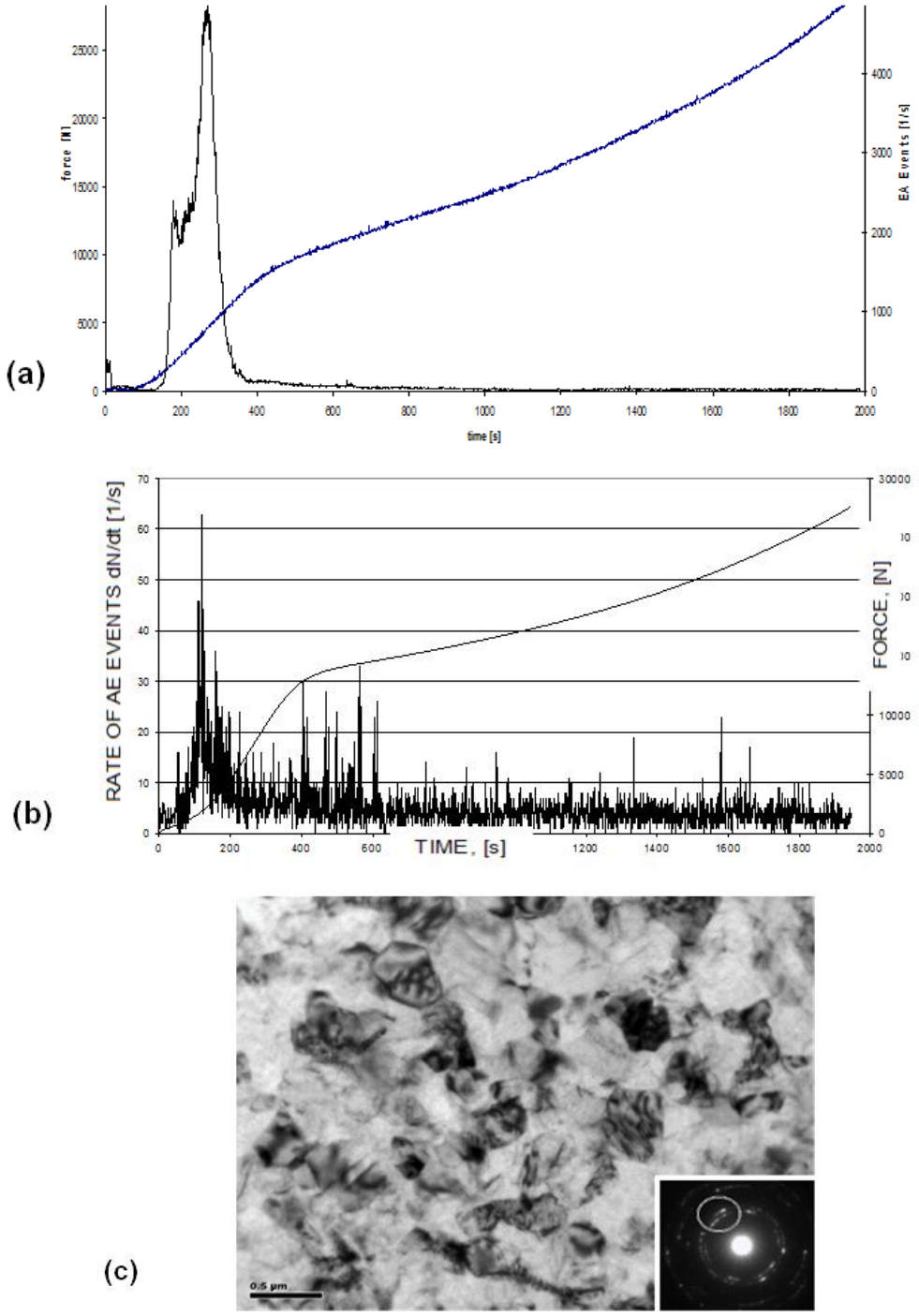

Fig. 3.22. Mg10Li sample before (a) and after (b) HPT processed three times together with appropriate TEM image (c).

The highest peak of AE event corresponds to the rate of order $2x10^3$/s (Fig. 3.26a) in the Mg12Li alloy and, which is characteristic, three distinct ranges of AE activity can be distinguished. The first, which is typical for the area of plasticity limit; the second, longer maximal one (at about 1500

up to 3000s) of order $9x10^2$/s and the third peak, the most active lasting from more than 3500s to the end of compression test (intensity about $2.5x10^2$/s).

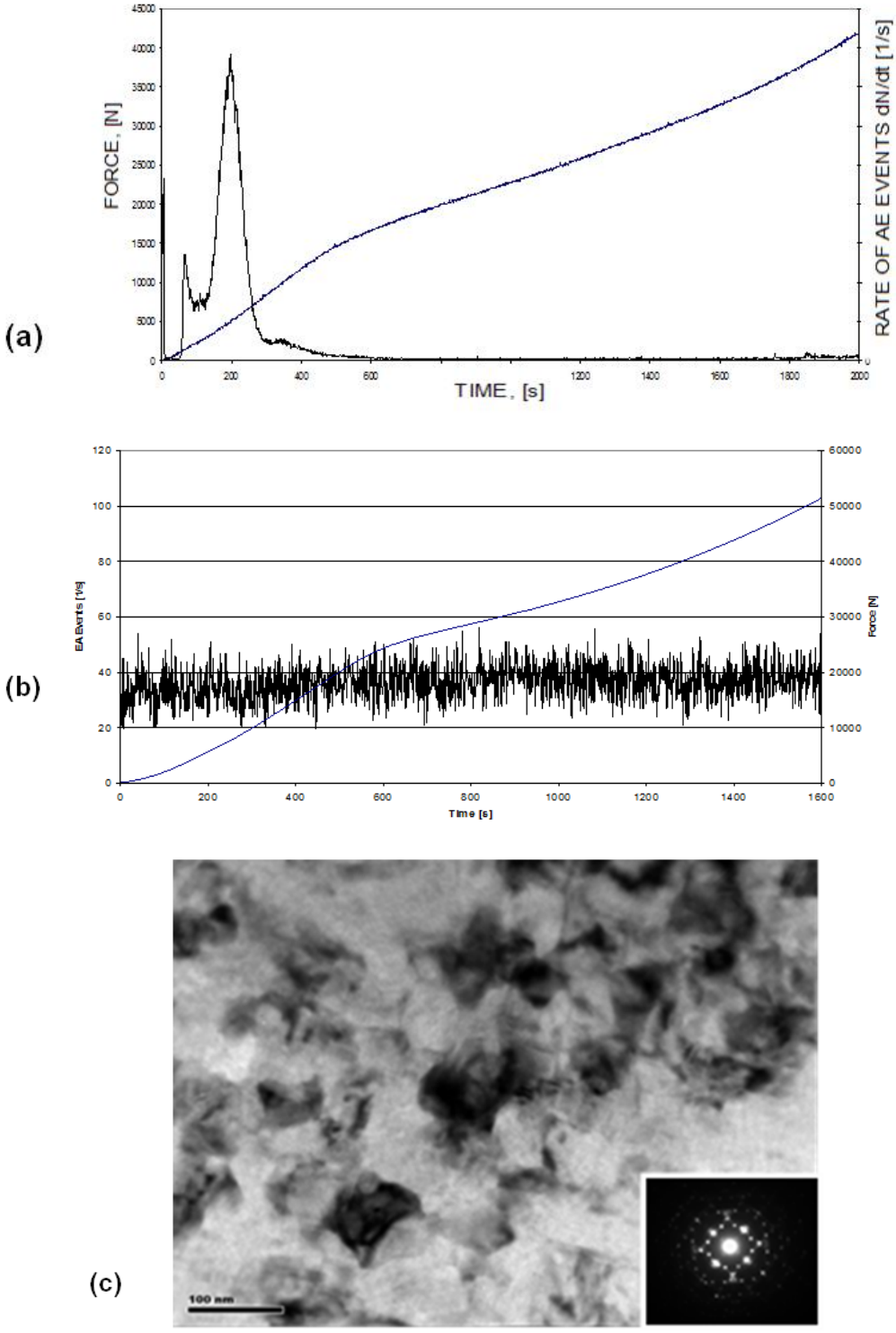

Fig. 3.23. AE event rate and compressive force of Mg10Li5Al sample prior to (a) and after 3-fold working with the HPT method (b) and respective TEM image (c).

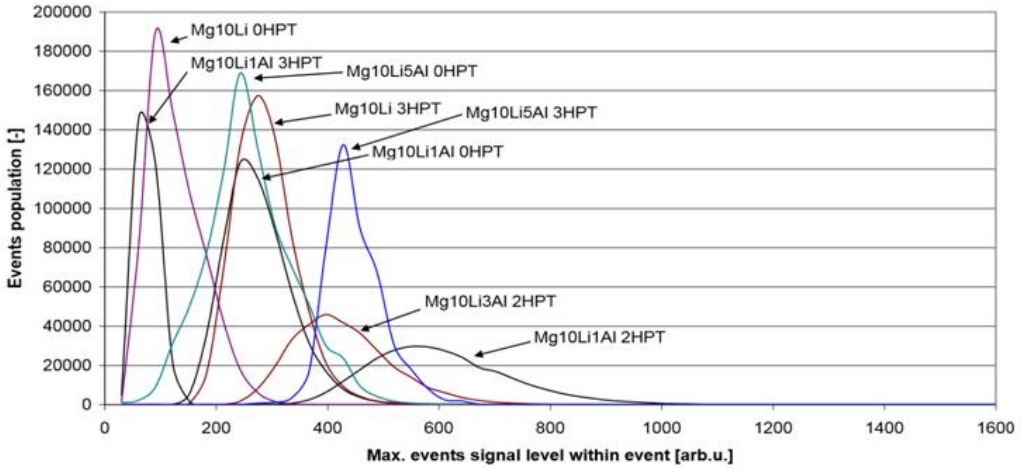

Fig. 3.24. Distributions of AE event number population in dependence on energy of examined alloys before and after processing with HPT method.

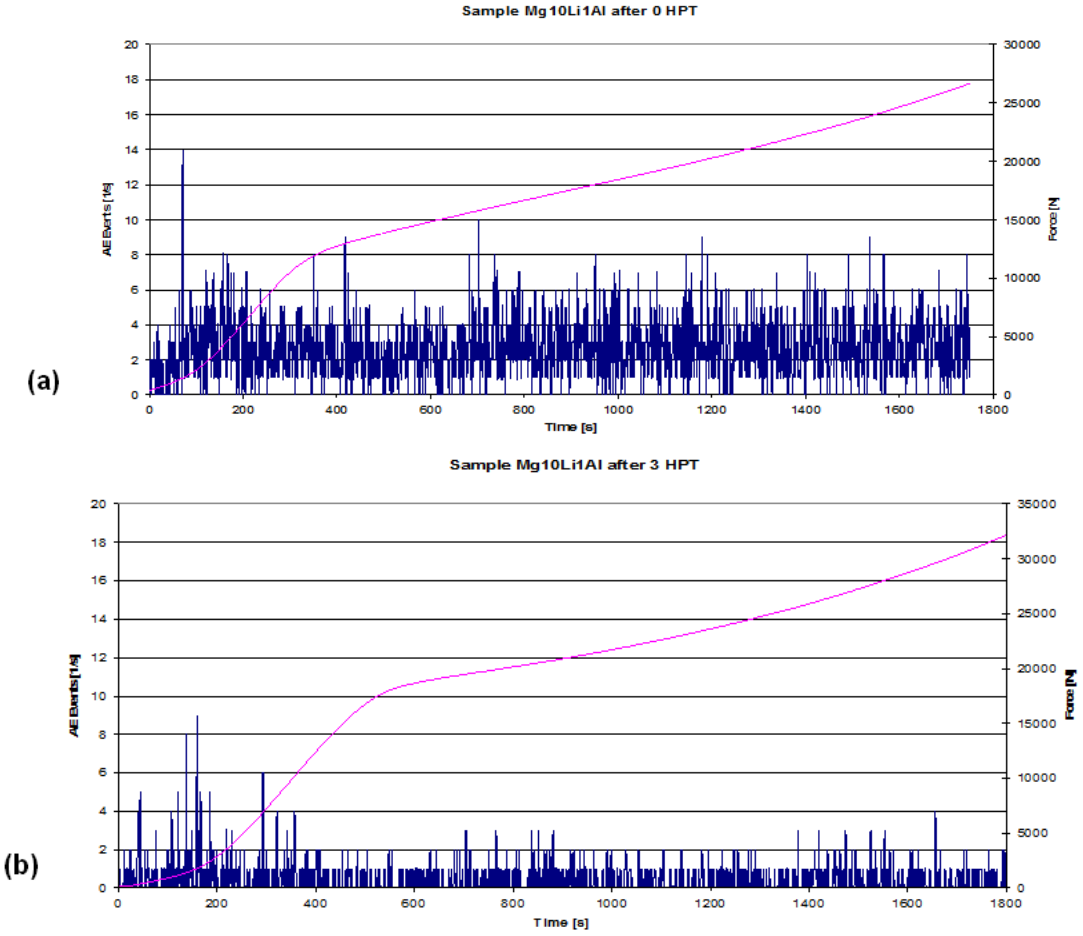

Fig. 3.25. AE and compression force in Mg10Li1Al before (a) and after 3-fold HPT processing (b).

It is unusual, that such a drastic decrease of AE level is, at the same time, bound with a very distinct increase of single β phase alloy plasticity. The specimens do not undergo destruction even after about 5000s of the test duration.

Considerable increase of plasticity with growth of lithium concentration may be explained by the activation of slip systems in (110) planes, characteristic for the A2 lattice (samples of single α phase alloys broke mainly slightly above (Fig. 3.2a) or slightly below 3000s (Fig. 3.3b). Based on the former discussion on two-phase alloys, it can be concluded that the β phase is weakly efficient acoustically. It can be said, that almost the whole weight of AE comes from the α phase, which is confirmed by the microstructure of Mg12Li5Al shown in Fig. 3.27b in comparison with that of α-Mg4Li5Al alloy (Fig. 3.3b lower part). The question, why the β phase is so weakly efficient acoustically, while the increase of lithium content promotes slip in (110) planes, which should rather lead to the increase of AE generated by dislocation processes, and not contrary to that what is being observed in this case. The answer can be sought based on diffusivity of lithium, which is very high, particularly in β-Mg8Li phase area and β-Mg12Li [32-35]. The extremely high diffusivity of lithium favors, among others, the formation of higher amount of vacancies, which in turn intensifies climbing the dislocations resulting in the increase of segments of dislocation lines, which do not lie in active slip planes. In consequence it limits to some extent the possibility of collective, synchronized movement of dislocation groups, which participates in the occurrence of measurable acoustic waves. A similar mechanism is also responsible for second and third range of AE activity in the β-Mg12Li alloy (Fig. 3.26a), because high plasticity of the alloys is due to a strong relaxation of strains during deformation [32-35] as the result of high diffusivity of lithium. The accumulation of internal strains takes place during acoustic silence e.g. in dense dislocation tangles followed by an intensive climbing of dislocations and cross slip, which results in violent synchronized annihilation of dislocation segments and contributes to the generation of small AE peaks. In consequence, it limits to a large extent the possibilities of collective, synchronized co-planar movements (in the common planes) of dislocations, which are necessary, so that measurable acoustic waves could appear. During the activity of AE emission, the density of dislocations and internal stresses decrease, followed by the acoustic silence. In consequence the process repeats periodically.

A strong effect of lithium is confirmed by the results of measurements of supersonic E Young's modulus and dumping coefficient α [24,28]. The E values changed within 40-48GPa for the Mg4Li and Mg8Li alloys, while they were confined to 19-27GPa for Mg12Li one, which is in satisfactory accordance with the observed mechanical properties of the alloys. However, the measurement of damping coefficient was reliable only for the Mg4Li alloy. For the remaining samples of higher Li content, the effect of Li on attenuation was so great, that the measurement result was unreliable.

The AE courses in Mg12Li3Al and Mg12Li5Al alloys are presented in Figs. 3.27a and 3.27b, respectively. In the case of Mg12Li3Al, after very short ranges of primary activity and some sporadically appearing AE impulses, acoustic silence (AE signals below the detection level) was observed, while the AE silence

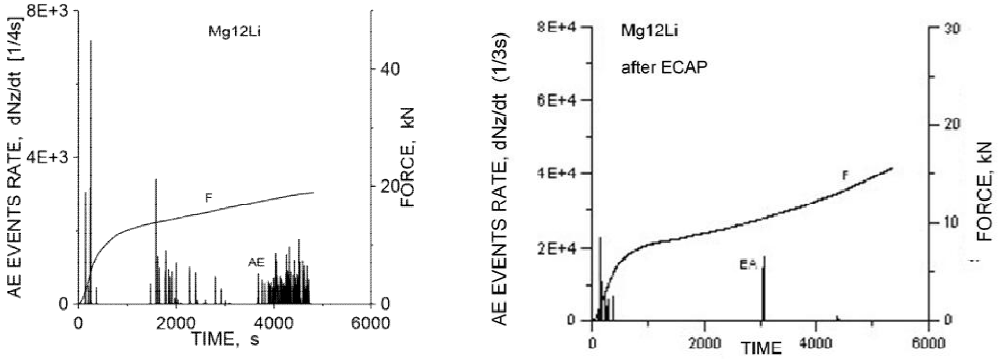

Fig. 3.26. AE and compression force of alloys based on β single phase subjected to tests of compression at room temperature; (a) - Mg12Li, (b) - Mg12Li after 4-fold ECAP operation.

in the Mg12Li5Al occurred already at about 500s. Such AE courses confirm the earlier findings that the β phase is very weak acoustically and on the other hand that the increase of Al concentration in the alloys based on the single matrix results in the decrease of AE rate and its activity. The curves confirm also very interesting phenomenon that such a drastic drop of AE intensity level is at the same time connected with the significant growth of plasticity of singe β phase alloys. As it was already mentioned, the samples do not undergo destruction even after 5000s duration of compression test.

The mechanical properties of the alloys are difficult to compare, because they are so plastic that the comparison of their courses of force during time up to 6000s cannot give reliable result. However, the measurements of E modulus confirm a greater strength of Mg12Li5Al (E=46.5MPa) than that of the Mg12Li3Al (43.5MPa) [24,28].

Based on above measurements of AE in the β single phase alloys of cubic lattice, it can be concluded that the behavior of AE is quite different and from the point of view physical reasons is by no means interesting (Fig. 3.26a). Instead, the behaviour of AE in these alloys subjected to 4-fold ECAP operation shown in Fig. 3.26b will be discussed below.

The comparison of the rate of AE events and external force during the compression test of pure Mg (99.99%) before (Fig. 3.1a) and after (Fig. 3.1b) singular extrusion in the angular channel ECAP as well as the behavior of AE and force in single-phase Mg12Li alloys before and after four-fold extrusion passes (Fig. 3.26a and b, respectively) allows the statement that the level of intensity in both cases drops after ECAP and the analysis of courses of external compressive force in samples after ECAP indicates the distinct elevation of plastic properties. It was confirmed by the results of compression tests of two-phase ($\alpha+\beta$) Mg8Li alloy before and after four-fold ECAP operation, respectively shown earlier in Part 3.2 in Figs. 3.4a and b. Moreover, the comparison of their microstructures before (Fig. 3.4a on the right) and after (Fig. 3.4b on the left) ECAP processing additionally illustrate very clear refinement of structure from grain size of a few hundred micrometers in the initial state up to some, several micrometers, which is achieved already after 4-fold processing in the angular channel.

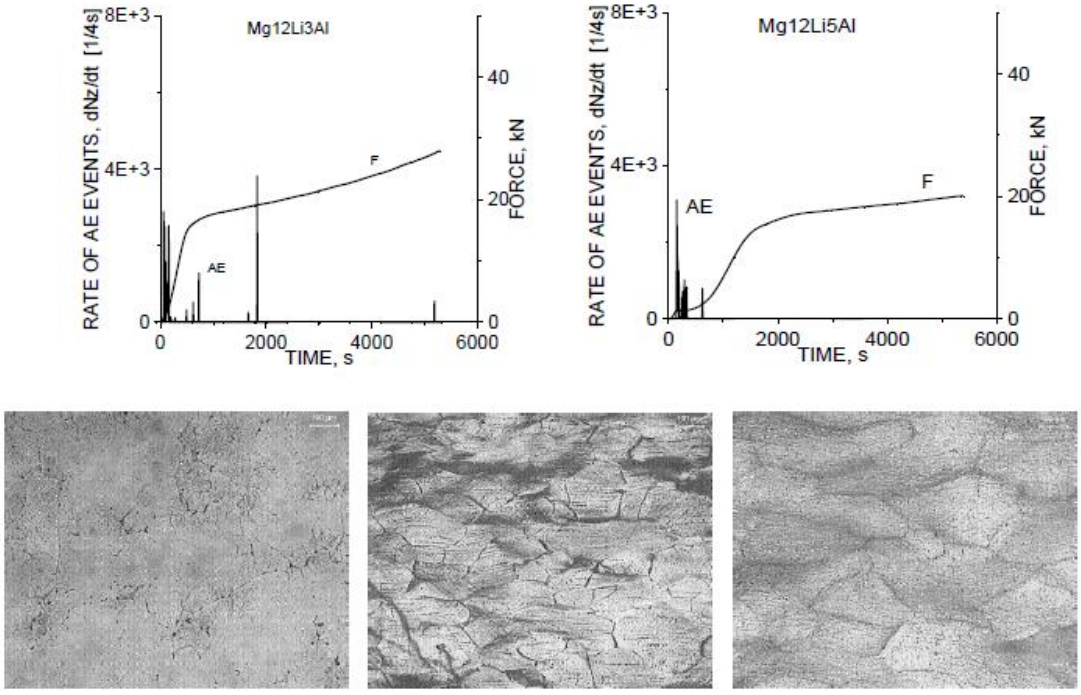

Fig. 3.27. AE in Mg12Li3Al (a) and Mg12Li5Al (b) alloys based on β phase and optical images of microstructure (from the left bottom side: Mg12Li3Al before and after deformation and deformed Mg12Li5Al alloy.

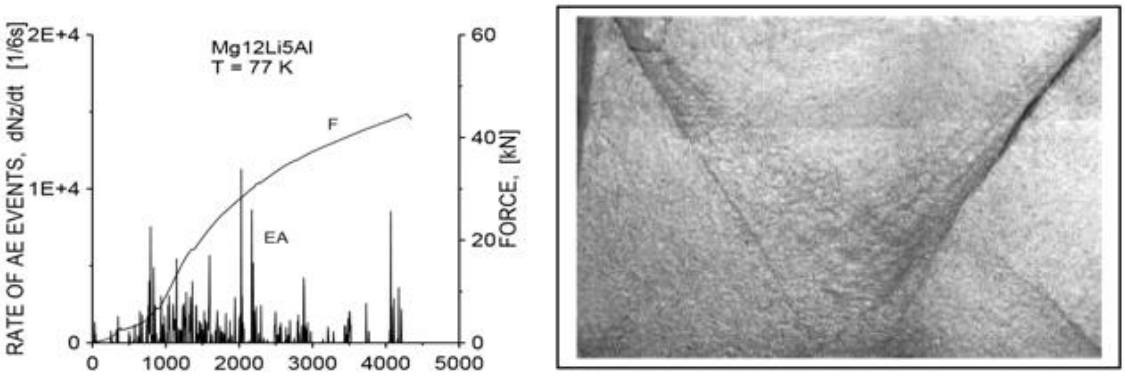

Fig. 3.28. Low temperature AE in Mg12Li5Al alloy (a) and corresponding microstructure (magnification x20), which illustrates primary and secondary family of shear bands (b).

3.3.2 Low temperature AE in alloys based on β phase

Due to the strong tendency to oxidation of the alloys based on β phase and in order to determine their resistance to changes of temperature the compression tests of Mg12Li5Al alloy at liquid nitrogen temperature (77K) were carried out for the first time. The results presented in Fig. 3.28 are so unexpected, that was is worth to pay attention to them. It came out that the β phase was not so weakly efficient acoustically, as it was at room temperature (Fig. 3.27b). The similar behavior of AE in both cases is connected with twinning, which occurred nearly from the beginning of the test. The formation of primary and secondary families of shear bands (Fig. 3.28b) manifested themselves with high AE peaks at the end of test. Moreover, the activity and intensity of AE at low temperature remain stable at distinctly high level (Fig. 3.28a) in comparison with its behavior at ambient temperature (Fig. 3.27b), at which it is below the discriminator threshold and is contained in the background of instrument noise. It is due to the fact that twinning at low temperature occurs almost from the beginning of test duration.

4. SUMMARY AND CONCLUSIONS

Phenomenon of acoustic emission (AE) and its relationships with mechanisms of deformations of Mg-Li and Mg-Li-Al alloys, taking place during channel compression before and after ECAP and HPT operations, was examined mainly at room temperatures. The Mg-Li alloys (Mg4Li, Mg8Li, Mg12Li) and Mg-Li-Al (Mg4Li3Al, Mg4Li5Al, Mg8Li3Al, Mg8Li5Al and Mg12Li3Al and Mg12Li5Al) were subjected to channel compression tests at room temperature only with the exception of Mg12Li5Al alloy which was tested also at liquid nitrogen temperature (77 K). Sporadically, channel compression tests were carried out for Mg8Li alloy after ECAP operation at 100°C.

The results obtained for pure polycrystalline Mg (99.99%), in which the level of event rate of order 10^4/s is connected with the area of yield point and microplasticity and prevalence of slips in the basal plane, were referential in the discussion. It was shown, that the basic contribution to the detected AE signals is a result of the collective, highly synchronized movements of dislocation groups related to the acceleration and internal, and mainly surface annihilation of many dislocations.

AE of α hexagonal Mg4Li, Mg4Li3Al and Mg4Li5Al alloys is almost two orders of magnitude higher than that of pure Mg and its event rate reaches the highest values, about $1.3x10^6$/s for the α single-phase Mg4Li alloy. Such a behavior of AE is imposed by the effect of Li addition, which decreases c/a parameter in the basal cell of HCP lattice and in this way favors additional slip systems in prismatic and pyramidal planes. The decrease of AE level in alloys containing Al comes from the presence of particles of LiAl or transition $MgLi_2Al$ phases, which to some extent restrain the movement and tendencies to collective activity of dislocations.

However, the AE values in α+β two-phase based alloys (Mg8Li, Mg8Li3Al, Mg8Li5Al) rapidly

decrease in relation to these of single α phase ones, although it is still twice as big (approx. 2-3x10^4/s) than in pure Mg. Such a violent drop of AE results from the β phase contribution, which is distinguished by particularly high diffusivity of lithium, which intensifies, among others, climbing of dislocations to other slip planes, which in consequence limits the possibilities of their collective behavior. In this point, the β phase is very weak acoustically. On the other hand, contrary to alloys based on the α phase, the AE level distinctly increases together with Al concentration. It is so, because the rise of Al concentration brings about the growth of α-phase volume fraction, which is very efficient acoustically.

Very weak acoustic efficiency of the β-phase is particularly visible in its alloys (Mg12Li, Mg12Li3Al and Mg12Li5Al), in which the AE level does not exceed the value of order 10^3/s. The occurrence of two ranges of AE activity is here characteristic, particularly in Mg12Li alloy, which also yield from the high diffusivity of Li, which facilitating the processes of internal stress relaxation ensures their high plasticity. A strong effect of lithium on AE was also confirmed with results of ultrasound measurements in the form of amplitude damping factor and Young's modulus [24,28].

Detailed microstructural examinations with the use of transmission electron microscopy (TEM) confirmed the occurrence of microstructure refinement from the initial grain size of order of few dozen micrometers down to below 1 μm for the HPT treated specimens, proving an ultra-fine grain character of intensive deformation. It was also so in the case of samples processed additionally with ECAP and observed in light microscopy technique.

The observed phenomenon of decrease of AE intensity and activity in materials subjected to HPT and ECAP processing may be explained in terms of two vital processes. One is connected with the strengthening mechanism during intensive deformation, when a distinct increase of dislocation density occurs compared with the initial state. In this way, the collective movement of dislocations generated during compression becomes strongly restricted due to intensive reaction of mobile dislocations with stationary forest ones. Another process is bound with the tendency to the increase of plasticity (or even superplasticity) in intensively deformed materials. In our earlier works [24,28-31], the following hypothesis was put forward. The drop of AE after severe processing takes place, because the slip along grain boundaries starts on the expense of typical dislocation slips in favored planes of crystallographic lattice in the area of individual grains, which is visibly less effective acoustically relative to efficient mechanism of collective and synchronized movement and annihilation of many dislocations. The verification of this problem is going to be undertaken in further research.

The obtained results allowed drawing some more important conclusions:

1. AE activity in Mg is connected with dominating slips in basal planes as the result of acceleration and surface annihilation of collectively moving dislocations.
2. High level of AE in α Mg4Li alloy is a result of additional slips in the prismatic and pyramidal planes.
3. The decrease of AE in (α+β) Mg8Li alloy is caused by β phase which is weakly efficient acoustically due to high Li diffusivity which, by enhancing relaxation processes, reduces the collective properties of moving dislocations.
4. AE in β Mg12Li alloy is by one order of magnitude smaller than that in Mg.
5. The effect of Al addition is related with the decrease of AE due to solid solution hardening by Al atoms in α phase and age hardening bY Li-Al particles in β phase which additionally restrict the collective slip of dislocations.
6. The AE increases together with Al concentration as the result of growing volume contribution of very efficient acoustically hexagonal phase.
7. Correlations of AE and deformation mechanisms may be interpreted on the ground of dislocation models and AE sources based on collective, synchronized processes of acceleration and annihilation of many dislocations, mainly surface annihilation.
8. The intensity and activity of acoustic emission significantly decreases in alloys compressed after processing with methods of intensive deformation (HPT, ECAP and ARB) in comparison with unprocessed alloys.
9. The AE decrease of alloys intensively processed is connected with considerable

refinement of structure and the tendency to growth of plasticity.

10. Degree of structure refinement is clearly higher as result of HPT processing than ECAP.
11. A hypothesis was put forward, that the decrease of AE in alloys compressed after intensive deformation results from the strengthening processes and the beginning of grain boundary slip.

ACKNOWLEDGEMENTS

The studies were financially supported in years 2009-2016 by the Polish Committee for Scientific Research (grant No 3 T08A 032 28) and by the Polish Ministry of Science and High Education (grant No N507 056 31/1289) by Polish National Science Centre (project in competition OPUS 4, grant No 2012/07/B/ST8/03055) as well as by the Grant Agency VEGA of the Slovak Republic (research projects No 2/0196/11 and No 2/0186/14).

Author desires also to thank Professors Zdzisław Jasieński, Andrzej Piatkowski and Zbigniew Ranachowski (form Polish Academy of Sciences) for very valuable cooperation during the realization of these studies. Thanks are belonged also to Doctors Stanislav Kudela and Stanislav Kudela Jr. from Slovak Academy of Sciences.

COMPETING INTERESTS

Author has declared that no competing interests exist.

REFERENCES

1. Valiev RZ, Ismagaliev RK, Alexandrov IV. Bulk nanostructured materials from severe plastic deformation. Progress in Materials Science. 2000;45:103-189.
2. Saito Y, Utsunomiy H, Tsuji AN, Sakai T. Novel ultra-high straining process for bulk materials – development of the accumulative roll-bonding (ARB) process. Acta Materialia. 1999;47:579-583.
3. Kuśnierz J. Microstructure and texture evolving under Equal Channel Angular (ECA) processing. Archives of Metallurgy. 2001;46:375-384.
4. Kuśnierz J, Pawełek A, Ranachowski Z, Piątkowski A, Jasieński Z, Kudela S, Kudela S Jr. Mechanical and Acoustic Emission Behavior Induced by channel-die compression of Mg-Li nanocrystalline alloys obtained by ECAP technique. Reviews on Advanced Materials Science. 2008;18:583-589.
5. Pawełek A, Bogucka J, Ranachowski Z, Kudela S, Kudela S Jr. Acoustic emission in compressed Mg-Li and Al alloys processed by ECAP, HPT and ARB methods, Archives of Acoustics. 2007;32: 87-93.
6. Kúdela S, Pawełek A, Ranachowski Z, Piątkowski A, Kúdela S Jr., Ranachowski, P. Effect of al alloying on the hall-petch strengthening and acoustic emission in compressed Mg-Li-Al Alloys after HPT processing. Kovove Materialy – Metallic Materials. 2011;49:271-277.
7. Pawełek A. Mechanical behavior and plastic instabilities of compressed Al metals and alloys investigated with application of intensive strain and acoustic emission methods, in the book: Recent Trends in Processing and Degradation of Aluminium Alloys. Published by InTech, Ed. Zaki Ahmad. 2011;Chapter 11:263-298.
8. Kúdela S. Mg-Li matrix composites – An overwiev. Int. J. Mat. Prod. Techn. 2003; 18:91-122.
9. Scott IG. Basic acoustic emission. Gordon and Breach, New York; 1991.
10. Wadley HNG, Scruby CB, Speake JH. Acoustic emission for physical examination of metals. Int. Metals Review. 1980;249: 41-64.
11. Kamado S, Kojima Y. Deformability and strengthening of superlight Mg-Li alloys. Met. Sci. Techn. 1998;16:45-54.
12. Pawełek A, Piątkowski A, Kudela S, Jasieński Z, Litwora A. Acoustic emission and mechanical properties of Mg-Li and Mg-Li-Al alloys subjected to channel-die compression tests. Molecular & Quantum Acoustics. 2002;23:351-362.
13. Pawełek A, Jasieński Z, Kudela S, Piątkowski A, Ranachowski P, Rejmund F. Acoustic emission in channel-die compressed Mg-Li-Al alloys reinforced with short ceramic fibres. 229-234; Influence of β phase on mechanical and acoustic behaviour of Mg-Li-Al alloys, 225-228, Proc Int. Conf. on Advanced Metallic Materials. Smolenice Castle, Slovakia, November 5-7; 2003.
14. Pawełek A, Bogucka J, Ranachowski Z, Kudela S, Kudela S Jr. Acoustic emission in compressed Mg-Li and Al alloys processed by ECAP, HPT and ARB

methods. Archives of Acoustics. 2007;32: 87-93.
15. Malecki I, Ranachowski J. Acoustic emission, sources, methods, applications, Ed. by PASCAL Publications – Committee of Scientific Research, Warsaw; 1994. (in polish)
16. Ranachowski Z. Methods of measurements and analysis of signal of acoustic emission, Scientific Works No 7/1997, Ed. by Institute of Fundamental Technological Research, Polish Academy of Sciences, Warsaw; 1997.
17. Pawełek A, Piątkowski A, Jasieński Z. Nonlinear and dislocation dynamics aspects of acoustic emission and microstructure evolution during channel-die compression of metals. Molecular and Quantum Acoustics. 1997;18:321-358.
18. Fisher RM, Lally JS. Can. J. Phys. 1967; 45:1147-1151.
19. Pawełek A, Piątkowski A, Jasieński Z, Pilecki S. Acoustic emission and strain localization in FCC single crystals compressed in channel-die at low temperature. Z. Metallkde. 2001;92:376-381.
20. Pawełek A, Kuśnierz J, Bogucka J, Jasieński Z, Ranachowski Z. Acoustic emission and the Portevin – Le Châtelier effect in tensile tested al alloys before and after processing by accumulative roll bonding, Franch-Polish Colloquium, Paris, France, May 20-21, 2008, Archives of Metallurgy and Materials. 2009;54:83-88.
21. Pawełek A. Dislocation aspects of acoustic emission in the plastic deformation processes in metals, Thesis (qualifying as assistant professor), 1-136, Institute of Metallurgy and Materials Science, Polish Academy of Sciences, Ed. OREKOP s.c., Cracow, Poland; 2006. (in polish)
22. Pawełek A, Malecki I. Acoustic emission and plasticity of crystals, Scientific Works No 22/1993, Ed. by Institute of Fundamental Technological Research, Polish Academy of Sciences, Warsaw; 1993. (in polish)
23. Pawełek A, Piątkowski A, Jasieński Z, Ranachowski P. Examination by acoustic emission methods of the resistance of ceramic and composite materials to compression and changes of temperature conditions, Report of the Committee of Scientific Research, Grant Nr 4 T08D 026 22, Cracow; 2005. (in polish)
24. Pawełek A, Piątkowski A, Ranachowski P, Ranachowski Z. Employment of acoustic method for estimate of the mechanical specificity of nanocrystalline alloys, composites and ceramic materials, Report of the Ministry of Science and Higher Educational, Grant Nr N507 056 31/1289, Cracow; 2010. (in polish)
25. Vinogradov A. Acoustic emission in ultra-fine grained copper. Scripta Materialia. 1998;39:797-805.
26. Kudela S, Trojanová Z, Kolenciak V, Lukác P. Short fibre reinforced Mg-8Li-xAl matrix composites – preparation, structure and properties, Proceeding of the Third International Conference on “Advances in Composites. Ed. E.S. Dwarakadasa and C.G. Krishnadas Nair, Bangalore. 2000; 679-686.
27. Trojanová Z, Drozd Z, Lukáč P, Kúdela S. Mat. Scie. Forum. 2003;419-422:817-824.
28. Jasieński Z, Pawełek A, Piątkowski A, Ranachowski Z. Application of the acoustic emission method for evaluation of plastic instability of metals and mechanical properties of nanocrystalline alloys and compo sites, Report of the Committee of Scientific Research, Grant Nr 3 T08A 032 28, Cracow; 2008. (in polish)
29. Pawełek A. The reasons for acoustic emission (EA) generation in Mg-Li and Mg-Al based alloys and composites subjected to compression tests before and after processing by intensive strain methods, Report of the Institute of Metallurgy and Materials Science, Polish Academy of Sciences, Cracow; 2011. (in polish)
30. Pawełek A. Examination of the reasons for acoustic emission (AE) generation in Mg-9Li based alloys and composites subjected to compression tests before and after processing by intensive strain methods, Report of the Institute of Metallurgy and Materials Science, Polish Academy of Sciences, Cracow; 2010. (in polish)
31. Pawełek A. Elaboration of identification manners of the plastic deformation mechanisms using optimized acoustic emission technique in compression tests of metals, alloys and composites before and after processing by intensive strain methods, Report of the National Science Centre, Cracow; 2013. (in polish)
32. Kuśnierz J, Pawełek A, Kúdela S, Piątkowski A, Mizera J, Ranachowski Z, Kúdela S Jr., Jasieński Z. Mechanical and

acoustic emission behaviour in compressed Mg-Li and Al alloys pre-deformed by intensive strain methods, The book of abstracts, pInt. Conf. ISPMA11, Prague, August 24-28. 2008;75.

33. Pawełek A. Possibility of a soliton description of acoustic emission during plastic deformation of crystals. Internal Report of the International Center for Theoretical Physics (ICTP), IC/87/136, Trieste. J. Appl. Phys. 1987; 1988:63:5320-5325.

34. Pawełek A. Density of kinks on a dislocation segment in the thermodynamic equilibrium and the interaction between solitons. J. Appl. Phys. 1987;62:2549-2550.

35. Kúdela S Jr., Wendrock H, Kúdela S, Pawełek A, Piątkowski A, Wetzig K. Fracture behaviour of Mg-Li matrix composites, The book of abstracts, p.73, Int. Conf. ISPMA11, Prague, August 24-28, 2008, International Journal of Materials Research. 2009;100:910-914.

Peer-review history:
The peer review history for this paper can be accessed here:
http://sciencedomain.org/review-history/20826